February 2009
Master's Thesis

Adsorption and Release Properties of Proteins on SBA-15 Nanoparticles Functionalized with Aminosilanes

Graduate School of Chosun University
Department of Chemical Engineering
Pham Thi Tra

Adsorption and Release Properties of Proteins on SBA-15 Nanoparticles Functionalized with Aminosilanes

February 2009

Graduate School of Chosun University

Department of Chemical Engineering

Pham Thi Tra

Adsorption and Release Properties of Proteins on SBA-15 Nanoparticles Functionalized with Aminosilanes

Aminosilanes를 함침한 기능성 SBA-15 나노 입자의 단백질의 흡착 및 탈착 특성

Advisor: Prof. Sun-Il Kim, Ph.D

Thesis submitted for the degree of Master

October 2008

Graduate School of Chosun University

Department of Chemical Engineering

Pham Thi Tra

Thesis submitted in partial fulfillment of the requirements for the degree of Master in the Graduate School Chosun University

Approved by the Guidance Committee:

Prof. Byung-Wook Jo
Chosun University _____

Prof. Sun-Il Kim
Chosun University _____

Prof. Jae-Wook Lee
Chosun University _____

November 2008

Graduate School of Chosun University

CONTENTS

LIST OF TABLES

LIST OF FIGURES

ABSTRACT

Adsorption and Release Properties of Proteins on SBA-15 Nanoparticles Functionalized with Aminosilanes

Pham Thi Tra

Advisor: Prof. Sun-Il Kim, Ph.D

Department of Chemical Engineering

Graduate School of Chosun University

Mesoporous silica materials have received much attention due to their attractive features, such as stable mesoporous structure, high surface area, large pore volume, regular and adjustable nano-pore sizes (2-10 nm). Among SBA (Santa Barbara Amorphous) materials, SBA-15 attracted researchers′ attention due to its prominent properties. Based on morphology of SBA-15 particles, each has its own synthesis procedure and characteristics, results in different adsorption capacity as well as application in drug delivery system. This study focused on the synthesis of mesoporous material SBA-15 with both rod-shaped and spherical morphology.

Mesoporous silica SBA-15 has been obtained via a two-step synthesis process (gel formation and subsequent hydrothermal treatment) by using a triblock copolymer as a template. Multi-amine-grafted mesoporous silicas SBA-15 were prepared by attaching 3-aminopropyltriethoxysilane, N-2(-aminoethyl)-3-aminopropyl trimethoxy silane and (3-trimethoxysilylpropyl) diethylenetriamine via post-synthesis method. The obtained

mesoporous silica SBA-15 were characterized by X-ray diffraction (XRD), transmission electron microscopy (TEM), scanning electron microscopy (SEM), fourier transform infrared (FT-IR), and BET analysis. The proteins used in adsorption experiments were Bovine Serum Albumin (BSA), Lysozyme (LYS) and Myoglobin (MYO). The protein adsorption properties such as equilibrium and kinetics were investigated. The results show that the original SBA-15 samples (R for rod-shaped and S2 for sphere) have the highest adsorption capacity for all proteins due to their largest pore size and internal surface area. Moreover, the release study of original and modified samples also were carried out to assess application for controlled drug delivery system. The adsorbed proteins can be readily desorbed on amine-modified samples. Especially, the diamine-modified sample (S2-AEAPS) has the highest release amount for two proteins, LYS and MYO.

국문초록

Aminosilanes를 함침한 기능성 SBA-15 나노 입자의 단백질의 흡착 및 탈착 특성

Pham Thi Tra
지도교수: 김선일 교수
생명화학공학과
조선대학교 대학원

메조포러스 실리카(Mesoporous silica)는 안정적인 구조, 높은 표면적, 높은 세공 부피와 규칙적인 세공 뿐만 아니라 세공크기(2~10 nm) 조절이 가능한 특성으로 인해 많은 관심을 받아 왔다. SBA 메조포러스 물질 중 SBA-15는 뛰어난 물성으로 인해 많은 연구자들로부터 관심을 받았다. SBA-15 입자들의 형태는 합성 과정 및 특성이 모두 다르기 때문에 그 흡착 특성 및 약물 전달 시스템 응용 분야 또한 모두 다르다. 본 학위논문에서는 막대 형태의 SBA-15와 구형의 SBA-15 메조포러스 실리카 물질 합성에 중점을 두었다.

SBA-15 메조포러스 실리카는 공중합 블럭(triblock)을 주형체(template)로 사용하여 2단계 합성 과정을 통해 얻었다. 아민이 함침된 메조 포러스 SBA-15를 얻기 위하여 3-aminopropyltriethoxysilane, N-2(-aminoethyl)-3-aminopropyl trimethoxy silane 과 (3-trimethoxysilylpropyl) diethylenetriamine를 SBA-15에 함침하였다. 제조된 샘플의 특성은 X선회절분석(XRD), 투과전자현미경(TEM), 주사전자현미경(SEM), FT-IR 및 BET 분석을 확인하였다. 흡착실험에 사용하기 위해 Bovine Serum Albumin (BSA), Lysozyme (LYS) 그리고 Myoglobin (MYO)의 단백질을 선정하여 흡착평형 및 속도론에 관한 흡착특성을 조사하였다. 실험

결과 함침을 하지 않은 막대 및 구형의 SBA-15 메조포러스 실리카의 경우 높은 세공 크기와 표면적으로 인해 선정한 모든 단백질에 대해 높은 흡착량을 보였다. 더불어 약물 전달 시스템에 적용하기 위해 아민 함침 유무에 따른 탈착 특성을 확인하였다. 아민이 함침된 샘플에 흡착한 단백질을 모두 쉽게 탈착시킬 수 있었다. 특히, diamine을 함침한 SBA-15 메조포러스 실리카(S2-AEAPS)는 LYS과 MYO 단백질에 대해 높은 탈착 성능을 보였다.

CHAPTER 1. INTRODUCTION

1.1. Mesoporous materials

Since the discovery of ordered mesoporous silica M41S by Mobil Oil researchers in 1992 [1,2], a variety of ordered mesoporous materials have been synthesized by using the template technique. The ordered hexagonal pore structure, high surface area, and inert framework of these materials have allowed use in a variety of applications including catalysis, separation, sensor design, nano-science and drug delivery system during the last decade. However, M41S materials are limited to a pore diameter of approximately 80 Å, and, furthermore, they have significant external surface areas. These characteristics limit use in size-selective separation of large biomolecules such as proteins and enzymes [4]. In 1998, the Stucky group synthesized the Santa Barbara Amorphous (SBA) materials by using neutral triblock template agents [3]. Among these SBA materials, SBA-15 attracted researchers' attention due to its prominent properties. This material was synthesized by Zhao et al. [9] using triblock copolymers (P123 or $PEO_{20}PPO_{70}PEO_{20}$) as a structure directing agent. The formation of the mesostructure is based on the synthesis pathway (S^0H^+) (X^-I^+) under acidic conditions (H^+X^-). The nonionic block copolymer (S^0) forms an organized structure due to self assembly of the template in aqueous solution. The process results in microphase separation and thus divides the space into hydrophilic and hydrophobic domains. The micelle formed during the self assembly consists of a core of hydrophobic block PPO and a shell of hydrophilic block PEO. Under acidic conditions, the self assembly is followed by the hydrolysis and condensation of silica source (TEOS) which results in the formation of inorganic (I^+) network of silica. The synthesis route is shown in Fig. 1.1. These copolymers have the advantage that their ordering properties can be changed by altering the solvent composition and the copolymer

architecture. Furthermore, thicker pore walls are obtained in SBA-15, compared to MCM-41, which improves the hydrothermal stability of these materials.

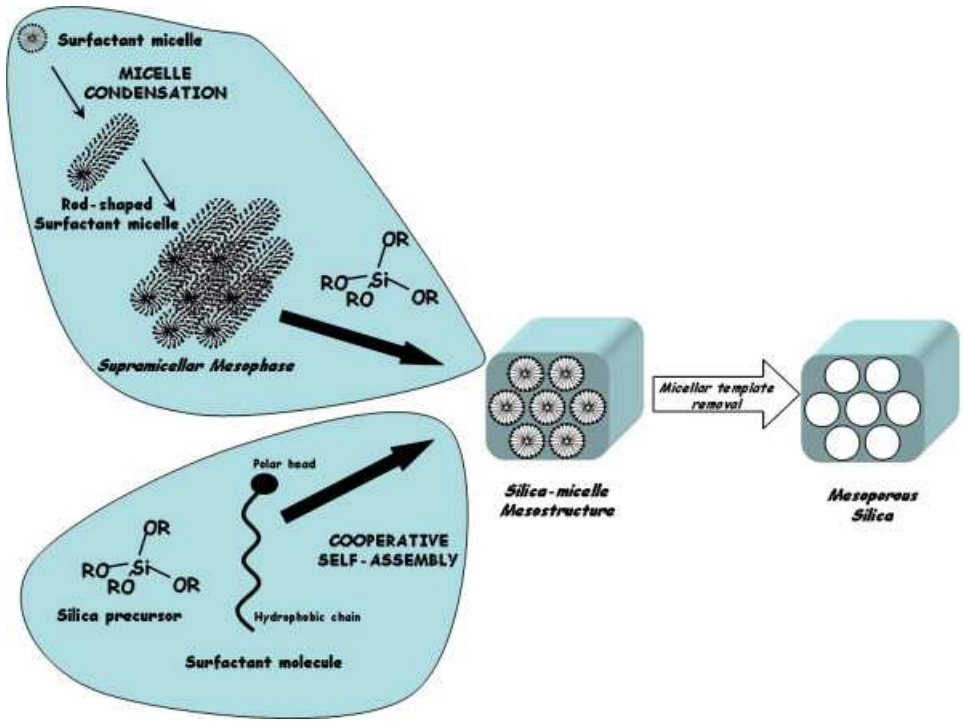

Fig. 1.1. Schematic representation of the two different mechanisms used to describe the synthesis of ordered mesoporous silica materials [34].

Many methods have been reported for controlling the pore size of mesoporous materials. The most frequently used procedure is the introduction of a swelling agent into the structure directing template. Common swelling agents are large organic hydrocarbons such as dodecane [30], 1,3,5-trimethylbenzene [31] and triisopropylbenzene [32]. The introduction of these agents has been shown to lead to the swelling of pore volumes of around 30%, but loss of long-range order of the mesoporous structure is observed. Other common methods have been reported such as mixing surfactant blends to tailor the pore size of mesoporous silicas, showing nanometer-level control over the pore diameters, although the longest surfactant chain governs the largest pore size achievable. In this study, the pore size of SBA-15 can be tuned by using swelling agents and controlling the aging time and temperature. As a result, SBA-15 is utility material for separating large biomolecules such as proteins and enzymes [5].

Particle shape has been shown to have an effect on the agglomeration and circulation properties of several non-porous nanoparticles in vitro. There are three methods that have been developed to tune the particle morphology of mesoporous silica materials. The first method involved the use of a series of antimicrobial room-temperature ionic liquids with various alkyl chain lengths as templates for the synthesis of mesoporous silica materials. The second method was based on a co-condensation reaction with TEOS and different organoalkoxysilanes. The effect of other co-condensing species on morphology was studied in detail, which enabled us to control the formation of mesoporous silica with different particle shapes. The third method to control particle morphology was done by tuning the ratios of reactants [38].

Modified silica materials with amine or other organic moieties have been widely used as fixed phases in high performance liquid chromatography (HPLC) [15,16], as adsorbents for the removal of organic compounds or metal ions from various sources [17,18] and as catalysts [19,20]. In some previous studies, multi-amine-functionalized mesoporous silicas have been

prepared and used to adsorb heavy metal ions and carbon dioxide [21,22]. There are two ways, including post-synthesis (grafting) and direct synthesis (co-condensation) methods to incorporate functional groups into the mesoporous matrix [23,24]. In post synthesis, organic functional groups are grafted through the reaction of a silane coupling agent with the free and germinal silanol groups on the surface of mesopores. The organic functional groups can be easily chosen and designed to meet different requirements. The resultant materials generally maintain highly ordered structures and show relatively high hydrothermal stability after grafting reaction. However, the distribution of the functional groups on the surface of the pore wall is likely not uniform and the organic groups are grafted mainly on the external surface of the mesoporous particles or near the pore mouth because of the mass transfer. Comparatively, the direct synthesis pathway by co-condensation of siloxane and organosiloxane precursors often offers a better control of the resultant materials in terms of a higher and more uniform surface coverage of the organic functionalities without the blockage of the mesopores. Nevertheless, the resultant materials usually show less structural ordering than the pure siliceous counterpart, and the organosiloxane precursors must be carefully chosen to avoid possible phase separation and Si-C bond cleavage during the synthesis and surfactant removal processes. To date, just several of the organic functional groups can be synthesized through the direct co-condensation method.

1.2. Drug delivery systems

Drug delivery is the method or process of administering a pharmaceutical compound to achieve a therapeutic effect in humans or animals. Drug delivery technologies are patent protected formulation technologies that modify drug release profile, adsorption, distribution and elimination for the benefit of improving product efficacy - safety and patient convenience -

compliance. Drug delivery technology is a multidisciplinary science involving the physical, biological, medicinal, pharmaceutical, biomedical engineering and biomaterial fields. Especially, chemists and chemical engineers have been interested in finding new material, controlling the rate and period of drug delivery, and targeting specific areas of the body for treatment. Recently, a new application of mesoporous silica as a drug delivery system has been explored owning to their non-toxic nature and good biocompatibility. In terms of drug delivery system, the development of mesoporous materials offers new possibilities for incorporating biological agents within silica samples and for controlling the kinetics of their release from matrix. One of the interesting features of mesoporous silica for controlled drug release is the multitude of possible modifications that can be used to both adjust surface functionality and change textural properties [37]. Functionalization by either co-condensation of organic species during synthesis or subsequent surface modification permits tuning surface properties, and thus could provide higher selectivity for specific controlled delivery.

1.3. Objectives

Based on morphology of SBA-15 particles, each has its own synthesis procedure and characteristics, resulting in different adsorption capacity as well as application in drug delivery system. This study focused on synthesis mesoporous material SBA-15 with both rod-shaped and spherical morphology.

Mesoporous silica SBA-15 has been obtained via a two-step synthesis process by using a triblock copolymer as a template. Multi-amine-grafted mesoporous silicas SBA-15 were prepared by attaching 3-aminopropyltriethoxysilane, *N*-2(-aminoethyl)-3-aminopropyl trimethoxysilane and (3-trimethoxysilylpropyl) diethylenetriamine via post-synthesis method. The characteristics of these samples have been analyzed by XRD, TEM, SEM, FT-IR and BET.

The protein adsorption properties such as equilibrium and kinetics were investigated. Moreover, the release study of initial samples and modified samples also were carried out to assess application for controlled drug delivery system. These proteins were Bovine Serum Albumin (BSA), Lysozyme (LYS) and Myoglobin (MYO).

This study is divided into 4 chapters. The first is Introduction, the next two chapters mention on SBA-15 mesoporous silica in both two morphologies such as rod-shape and sphere. The final chapter is Overall Conclusion.

CHAPTER 2. ROD-SHAPED SBA-15

2.1. Introduction

One of the main areas of interest in materials chemistry is the synthesis of mesoporous molecular sieves with highly controllable morphologies for the purpose of providing catalytic, separation, and adsorption applications to industry. Nonionic templates such as poly(ethylene oxide) (PEO) and block copolymers have received a great deal of attention in the synthesis of mesoporous materials because of their ability to self-assemble into well-defined mesophases with crystalline-like long-range orders. Furthermore, such nonionic surfactants are easily separated, nontoxic, biodegradable, and relatively inexpensive. The $[S^oH^+][X^-I^+]$ assembly pathway using block copolymer templating has resulted in various morphological mesoporous silicas arising from weak interface interactions mediated by the X^- anions under conditions, like in the $S^+X^-I^+$ assembly pathway using a cationic surfactant.

In this chapter, rod-shaped SBA-15 particles were synthesized by using Pluronic P123 triblock copolymer ($PEO_{20}PO_{70}PEO_{20}$) as a structure-directing agent and tetraethyl orthosilicate (TEOS) as a silica source. We controlled the pore size of SBA-15 by using swelling agent at different conditions of aging such as temperature and time. As a result, the largest pore size SBA-15 nanoparticles were obtained. Multi-amine-grafted mesoporous silicas SBA-15 were prepared by attaching 3-aminopropyltriethoxysilane, N-2(-aminoethyl)-3-aminopropyltrimethoxysilane and (3-trimethoxysilylpropyl)diethylenetriamine via post-synthesis method. The protein adsorption properties were investigated by Langmuir equation. Moreover, the release study of initial samples and modified samples also were carried out under neutral pH condition.

2.2. Experimental

2.2.1. Materials

The chemicals used in this study include: pluronic P123 triblock copolymer (poly(ethylene glycol)-block-poly(propylene glycol)-block-poly(ethylene glycol), MW:5800, Aldrich), tetraethyl orthosilicate (TEOS, 98%, Sigma-Aldrich), hydrochloric acid (35-37%, Junsei), mesitylene (1,3,5-trimethylbenzene, 98%, Aldrich), sodium azide (Junsei). The various aminosilanes used as grafting agents were 3-aminopropyltriethoxysilane ($H_2NCH_2CH_2CH_2Si(OCH_2CH_3)_3$, abbreviated as APTES, 99%, Aldrich), N-2(-aminoethyl)-3-aminopropyltrimethoxysilane (or N-[3-(trimethoxysilyl)propyl]-ethylenediamine, $H_2NCH_2CH_2$ $NHCH_2CH_2CH_2Si(OCH_3)_3$, AEAPS, 97%, Aldrich), N^1-[3-(trimethoxysilyl) propyl]diethylene triamine ($H_2NCH_2CH_2NHCH_2CH_2NHCH_2CH_2CH_2Si(OCH_3)_3$, TA, tech, Aldrich). Three proteins were Bovine Serum Albumin (BSA, A-3912, Sigma Aldrich), Lysozyme (LYS, L-6876, Sigma Aldrich), and Myoglobin (MYO, M-0630, Sigma Aldrich).

2.2.2. Synthesis of rod-shaped SBA-15

Rod-shaped SBA-15 was synthesized by a procedure similar to that described previously [25], via two-step synthesis: gel formation and subsequent hydrothermal treatment. An initial gel formation was done under acidic conditions using Pluronic P123 triblock copolymer ($PEO_{20}PO_{70}PEO_{20}$, Aldrich) as a structure-directing agent and tetraethyl orthosilicate (TEOS, Aldrich) as a silica source. In the specific procedure, 4 g of P123 is dissolved completely in 104 g of deionized water and 20 mL of fuming HCl (37%) added under stirring condition for 2 h. TMB was used, in an appropriate ratio with the surfactant, as a swelling agent for increasing the pore size. Next, 8.56 g of TEOS was added drop wise and the mixture was vigorously stirred for 24 h at 35 ^oC. The synthesized gel was then transferred into

heatproof plastic bottle at different temperatures and periods of time depending on targeted pore size. The solid products were filtered, washed with distilled water repeatedly and dried at room temperature overnight. The powdery SBA-15 was obtained by calcination in ambient air from room temperature to 550 ^{o}C, with a heating rate of 1 ^{o}C/min. The temperature was held constant at 550 ^{o}C for 6 h, the cooling rate was 5 ^{o}C/min.

2.2.3. Modification of SBA-15

Modified mesoporous materials with aminopropyl groups have alternatively been prepared by refluxing freshly activated mesoporous silica in toluene solution containing aminosilane. 5.0 g of calcined rod-shaped SBA-15, which was previously dried at 125 ^{o}C for 6 hours in air, was refluxed in the toluene solution of aminosilane (1.7%, 250 mL) at 110 ^{o}C for 24 hours under an Ar flow. The amine-functionalized SBA-15 was collected by filtration, washed with dry toluene, and dried at 60 ^{o}C overnight [22]. These materials are designated as R-APTES, R-AEAPS and R-TA, where APTES, AEAPS and TA are 3-aminopropyltriethoxysilane, *N*-2(-aminoethyl)-3-aminopropyltrimethoxysilane, and N^1-[3-(trimethoxysilyl)-propyl]diethylene triamine, respectively.

2.2.4. Characterization

X-ray diffraction (XRD) patterns were obtained on a PANalytical (Philips) X′Pert PRO MRD diffractometer using Cu Kα radiation source of wavelength 1.5406 Å for 2theta ranging from 0.01^{o} to 5^{o} with a scan speed of 3.0^{o}/min at 40kV and 30 mA. Nitrogen physisorption isotherms were measured on a micromeritics ASAP 2020 analyzer at 77K. The specific surface areas were evaluated using Brunauer-Emmett-Teller (BET) method. The pore size distribution was calculated using the Barrett-Joyner-halenda (BJH) method based on the

adsorption branch of the isotherms, and the pore size was reported from the peak position of the distribution curve. The pore volume was taken at the *P/Po* = 1.00. Transmission electron microscopy (TEM) was performed on a Hitachi H-7100 electron microscope, operating at 75kV. The scanning electron microscopy (SEM) was carried out on a Hitachi S-800 electron microscope. Fourier Transform Infrared (FT-IR) spectra of mesoporous materials before and after modification were observed by using FT-IR-410 Jasco.

2.2.5. Protein adsorption and release study

Protein adsorption was measured by the classical batch equilibration method. Batch adsorption experiments were carried out by contacting 50 mg of SBA-15 with 10 mL of different protein concentrations in buffer solution at 25 ^{o}C. In order to prevent microbial contamination, sodium azide was added into the solution. The adsorbent and solution were sealed and kept in a shaking incubator at 250 rpm for 24 h. The supernatant was diluted in a buffer and then filtered through 0.2 μm HT Tuffryn low protein binding membrane filters. The protein concentration in the supernatant was analyzed on a UV spectrophotometer with wavelength of 280 nm. A mass balance was applied to calculate the protein adsorbed on the SBA-15.

In order to investigate the release kinetics of proteins, the experiments were performed as follows. 100 mg of treated SBA-15 was soaked in 20 mL of neutral phosphate buffer solutions. The temperature was maintained constantly at 37 ^{o}C and the solutions were continuously shaked with a speed of 250 rpm. Samples of 3 mL were withdrawn from dissolution medium at appropriate time intervals and replaced with an equal volume of dissolution medium to maintain perfect sink conditions. The cumulative release amount was determined by a mass balance equation similar to the previous section.

2.3. Results and discussion

2.3.1. Characterization of rod-shaped SBA-15

The synthesized SBA-15 samples R, R-APTES, R-AEAPS and R-TA were characterized by XRD. Fig. 2.1 shows the XRD patterns of these samples. The first diffraction peak is clearly observed in R, which could be indexed as (100) diffraction peak associated with *p6mm* hexagonal symmetry. For R-APTES, R-AEAPS and R-TA, the intensities decrease drastically compared to that of R because of incorporating amine group onto the original sample R. After attaching the amine functional groups onto the silica surface, the XRD patterns changed. No peak is found in the XRD patterns of modified rod-shaped SBA-15. According to the previous studies, the XRD pattern of conventional SBA-15 was obtained from 1^o to 7^o of 2θ [3, 27]. In this work, we want to get a target sample with the large pore size by controlling aging conditions and using swelling agent. Hence, the peak of sample R was changed a little in position, but it still characterizes the *p6mm* hexagonal symmetry.

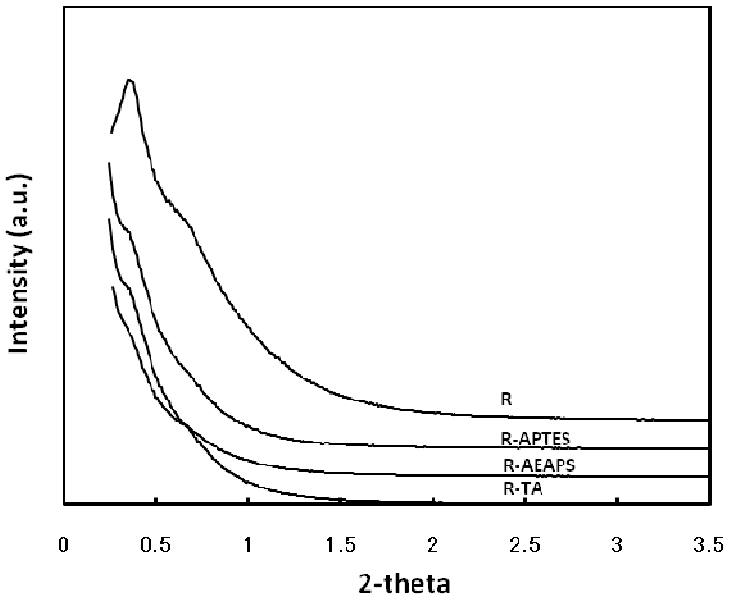

Fig. 2.1. XRD patterns of rod-shaped SBA-15 samples

The TEM image shows the very well-ordered hexagonal structure of original SBA-15. The conventional SBA-15 possesses very long rod-shaped material, but the SEM image, which is shown in Fig. 2.2, indicates the SBA-15 after controlling the pore size to be unshaped material. Obviously, the presence of TMB causes an increase in the pore size and a more amorphous morphology [36].

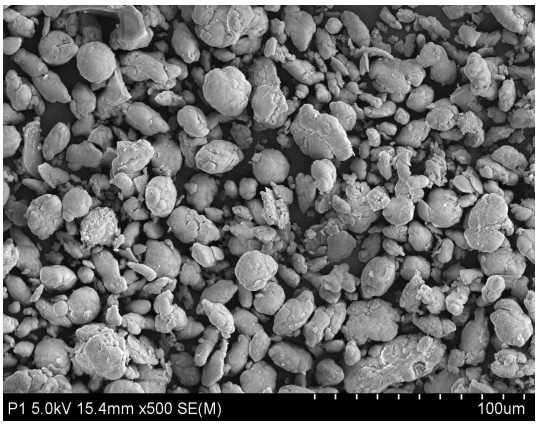

Fig. 2.2. SEM image of rod-shaped SBA-15

Fig. 2.3 shows the pore size distribution and the nitrogen physisorption isotherms of original SBA-15 sample R, which gives a typical irreversible type IV isotherm with a H_1 hysteresis loop as defined by IUPAC [26]. The nitrogen adsorption at low relative pressures (*P/Po*<0.1) is accounted for by monolayer adsorption of nitrogen on the pore walls, and does not necessarily imply the presence of micropores. The sharp inflection in the *P/Po* range from 0.6 to 0.8 of the isotherm is characteristic of capillary condensation within uniform mesopores, the position of which is clearly related to a diameter in the mesopore range. The pore volume and the surface area of the amine-grafted samples significantly decrease as compared with that of original SBA-15. The more amino groups or longer chain the silane coupling agents have, the smaller the pore diameter is and the lower surface area and pore volume are [21]. The BET

surface area and average pore volume of rod-shaped SBA-15 are 658 m^2g^{-1} and 1.08 cm^3g^{-1}.

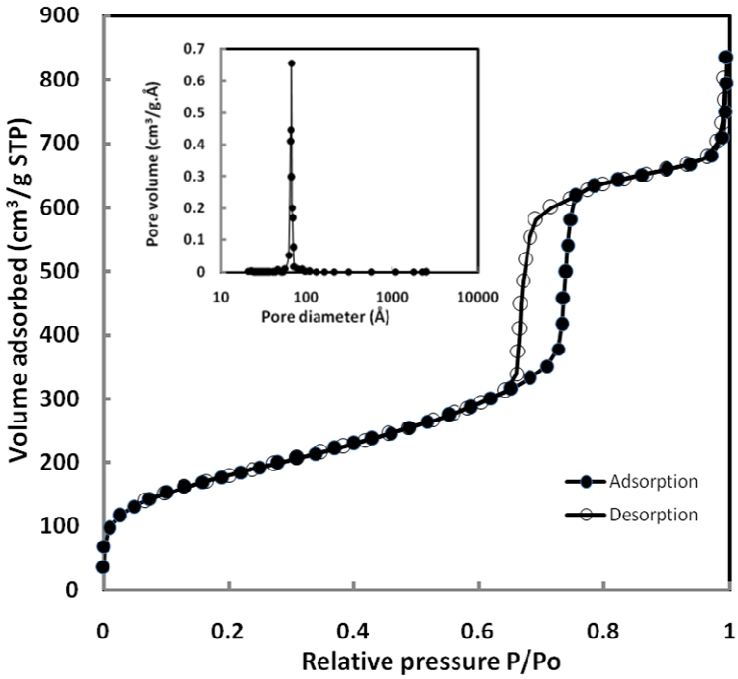

Fig. 2.3. Nitrogen adsorption and desorption isotherms and pore size distribution of rod-shaped SBA-15

Fig. 2.4 shows the infrared spectra of SBA-15 before (R) and after modification (R-APTES, R-AEAPS and R-TA). There are several bands appearing in the amino-functionalized SBA-15. In fact, it is difficult to determine the functional group $-NH_2$ attached on the surface mesoporous material by observing peak around 3460 cm^{-1} because the band of $-NH_2$ overlaps with that of O-H stretching vibration [5]. The appearance of peaks at 1560 cm^{-1} corresponds to the N-H (primary amine) bending vibration. It confirms the presence of $-Si(CH_2)_3NH_2$ functional groups on the wall surface [39].

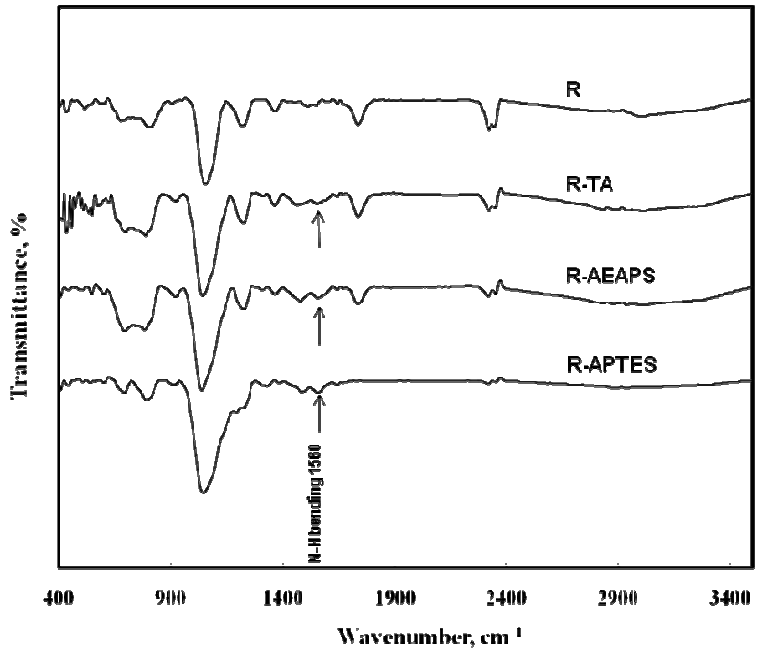

Fig. 2.4. IR spectra of rod-shaped SBA-15 sample functionalized with aminosilanes

2.3.2. Protein adsorption and release study

Because the pI values of BSA, LYS, MYO are 4.8, 11 and 7, respectively, the protein adsorption experiments were carried out at 25 ^{o}C and pH values of 4.8, 11 and 7. The isoelectric point is the pH value in solution at which the sum of charges on the protein is zero. The protein molecular is positively charged at a pH below the pI. On the contrary it is negatively charged at a pH above the pI. The properties of BSA, LYS and MYO are shown in Table 2.1.

Table 2.1. Physical properties of proteins [27]

Proteins	Molecular weight	Isoelectric point	Molecular size (Å)
BSA	69,000	4.7-4.9	40 x 40 x 140
Lysozyme	14,400	11	30 x 30 x 45
Myoglobin	17,600	7.0-7.2	25 x 35 x 45

The amount of protein adsorbed, q_t (mg/g) at any intermediate time, t was calculated from the mass balance equation as follows:

$$q_t = \frac{(C_o - C_t)V}{m} \quad (1)$$

where C_o is the initial concentration of solution (mg/mL), C_t is the concentration of solution at time t (mg/mL), V is the volume of solution (mL) and m is the mass of adsorbent (g).

In order to investigate the properties of protein adsorption on SBA-15, the isotherm

model Langmuir was applied.

$$q_e = \frac{q_m K_L C_e}{1 + K_L C_e} \tag{2}$$

In equation (2), q_e is the equilibrium adsorption amount (mg/g); q_m is maximum adsorption capacity (mg/g); K_L is the Langmuir constant and C_e is equilibrium concentration of solute (mg/mL).

The isotherm parameters were determined by minimizing the mean percentage deviations between experimental and predicted amount adsorbed, based on a modified Levenberg-Marquardt method (IMSL routine DUNSLF). The object function, *E(%)*, represents the average percent deviation between experimental and predicted results as follows:

$$E(\%) = \frac{100}{n} \sum_{k=1}^{n} \left[\frac{\left| q_{\exp,k} - q_{cal,k} \right|}{q_{\exp,k}} \right] \tag{3}$$

In equation (3), n is the number of experimental data, $q_{\exp,k}$ is the experimental adsorption capacity, and $q_{\mathrm{cal},k}$ is the calculated adsorption capacity. The isotherm data were fitted with Langmuir equation very well. The determined isotherm parameters of proteins on SBA-15 are listed in Table 2.2.

Table 2.2. Langmuir isotherm parameters of proteins (for rod-shaped SBA-15).

Protein	SBA-15 samples	q_m	b	*E(%)*
BSA	R	863.57	5.48	1.58
	R-APTES	790.00	1.58	1.75
	R-AEAPS	778.70	0.29	3.79
	R-TA	913.71	0.13	6.62
LYS	R	51.56	0.80	4.82
	R-APTES	10.56	0.53	6.93
	R-AEAPS	12.39	3.99	2.70

	R-TA	7.11	13.38	1.29
MYO	R	243.31	62.91	5.07
	R-APTES	37.14	0.46	9.31
	R-AEAPS	21.33	2.98	7.39
	R-TA	21.46	1.51	6.18

Fig. 2.5 shows the adsorption isotherms of BSA, LYS and MYO on SBA-15 at 25 ^{o}C. The sample which has the highest adsorption capacity for all proteins is the original sample R due to its largest pore size and internal surface area. After attaching of functional groups onto the surface, the adsorption amounts of R-APTES, R-AEAPS and R-TA were decreased due to a significant decrease in pore size and surface area. For BSA, the adsorption capacity is decreased with increase in amine group amount attaching onto original SBA-15 surface. The R-TA sample has the lowest adsorption capacity at the same condition considered with others. This result was in accordance with previous study [5], related to BSA adsorption onto SBA-15 samples before and after modification. There are some differences in adsorption capacity of SBA-15 samples between proteins. For LYS and MYO, the sample which has the lowest adsorption capacity is R-APTES (not R-TA as for BSA). The largest pore size of R compared to the modified samples is a very good candidate for separation of large size biomolecules, i.e BSA. Compared with some previous reports [27, 36], although the pore size of R is smaller than that of their samples, the adsorption capacity of R is very high because of the large surface area. The interactions between proteins and SBA-15 sample R are both chemical bond and physical bond (hydrophilic interaction), due to the presence of hydroxyl groups on the surface of SBA-15 and the functional groups of proteins. After modification via post synthesis, the hydroxyl groups on surface of silica are partially lost because of high temperature

hydrothermal and calcination treatment. Moreover, the attachment of nonpolar and hydrophobic methyl groups in grafted chains made the surface of SBA-15 more hydrophobic and a decrease in pore size. Hence, the amount of proteins adsorbed on the amine-modified sample is reduced in comparison to that before modification [5].

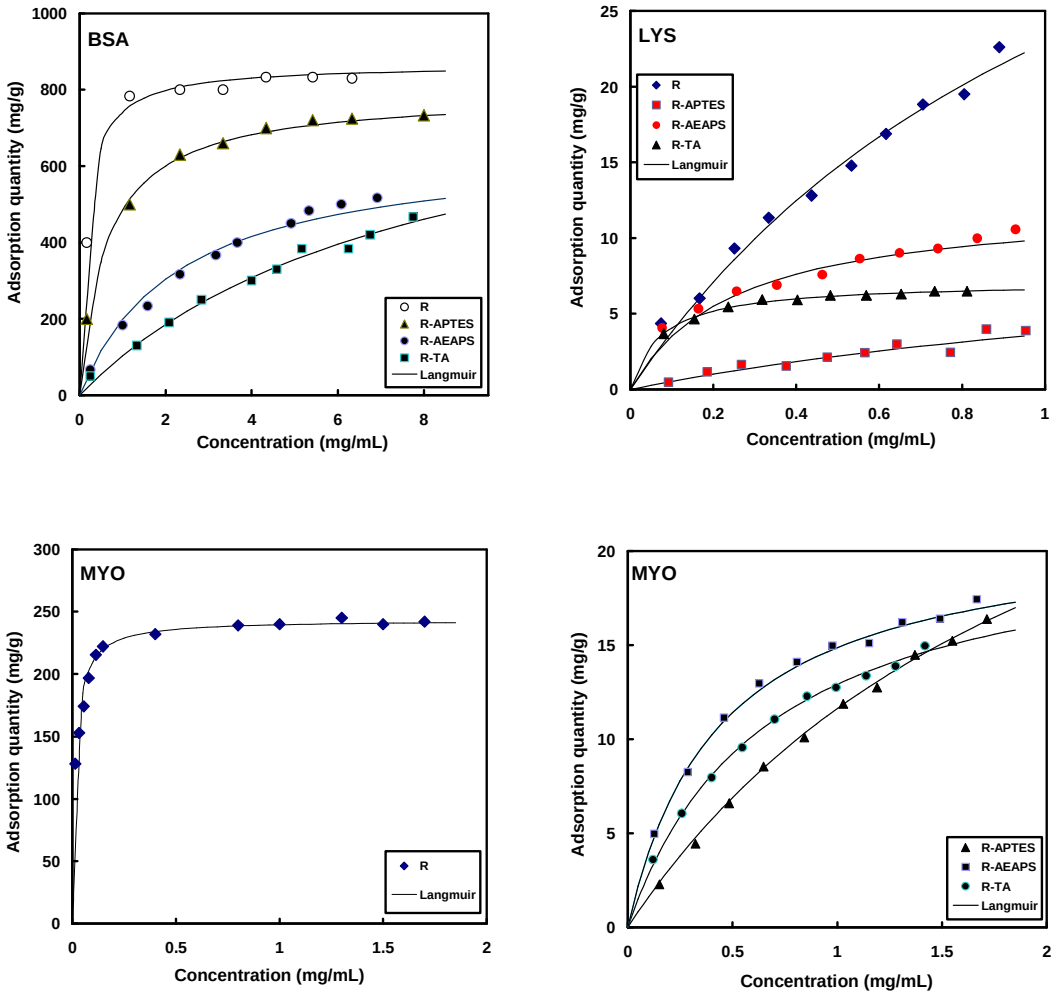

Fig. 2.5 Adsorption isotherms of BSA, LYS and MYO on rod-shaped SBA-15

Fig. 2.6 shows the release amount of proteins for all SBA-15 samples. Although the adsorption capacity of R was highest among all samples, the amount released by R-APTES, R-AEAPS and R-TA was higher than that of R in neutral solution for all proteins. In comparison between proteins, the release amount of LYS is lowest for all samples. According to the results of Song et al, the release rate of BSA from amine-modified SBA-15 via post synthesis was very high and all the adsorbed protein could be released completely after 3 hours. However, the loading amount of BSA on their modified sample chosen to carry out the release study was only 1.5 wt% at pH 4.8 because of the small pore size and BET surface area [24]. Thus, most of protein molecules adsorbed on the external surface of SBA-15 could be easily desorbed.

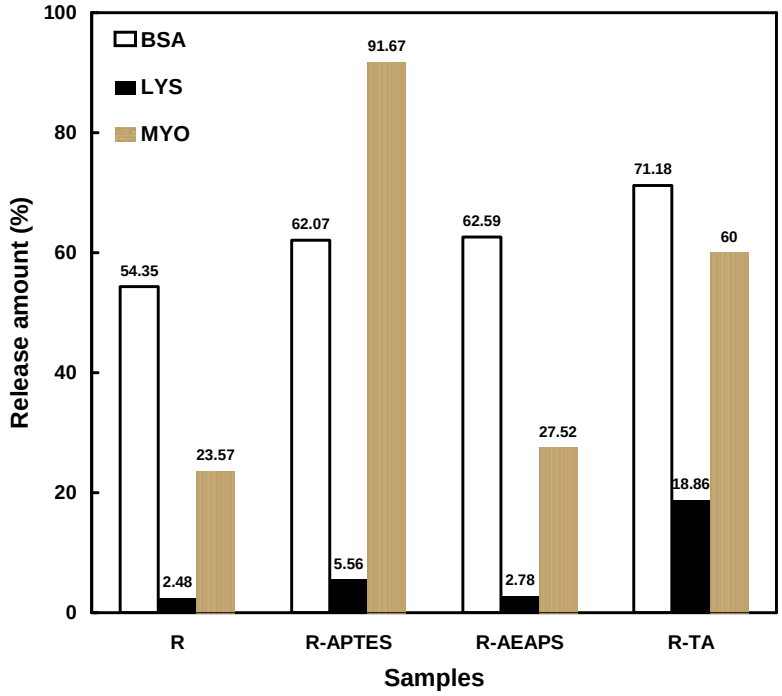

Fig. 2.6. Release amount of proteins for rod-shaped SBA-15

2.4. Conclusion

In this chapter, we have made the rod-shaped SBA-15 sample with the large pore size by using swelling agent under certain conditions, i.e. at high aging temperature and prolonged aging time. In addition, the surface characteristics of SBA-15 can be modified by incorporating amine functional groups via post synthesis method. The adsorption equilibrium of BSA, LYS and MYO on conventional and amine-modified SBA-15 reaches the maximum value at the pI of proteins because the lateral repulsion between adsorbed proteins is minimal. The original rod-shaped SBA-15 has the highest adsorption capacity for all proteins due to its largest pore size and internal surface area. The isotherm data fitted very well with Langmuir equation. It was also found that the adsorbed proteins can be readily desorbed in the neutral solution on amine-modified samples. Thus, the modified samples can be applied for controlled drug delivery system.

CHAPTER 3. SPHERICAL SBA-15

3.1. Introduction

The morphological control is one of the main subjects in this rapidly developing research field because the overall morphology is as important as the internal structure of a mesoporous material for certain applications. Recently, the disclosure of mesoporous SBA-15 sparked off considerable interest for its larger pore size, thicker wall and better stability. The most common morphology of SBA-15 are fiber-like several tens of micrometers in length, composed of “basic” rod-like particles, or individual well-defined rod-like particles [6,7,8]. Other morphologies with doughnut, rope, egg, sausage, sphere, discoid, and hyperbranched shapes of SBA-15 materials have been obtained, using organic reagents, strong electrolytes, or metal ions as additives [9,10]. Among various morphologies, spheres are required as column packing materials and easy-to-handle forms in certain applications such as chromatographic separations and controlled drug delivery [11,12,13]. Mesoporous SBA-15 materials with nearly spherical shapes have been prepared by using triblock copolymer with cetyltrimethyl-ammonium bromide (CTAB) as co-surfactant or through controlling the synthetic temperature at 20 ^{o}C [6]. Lee et al. synthesized nearly sphere-shaped SBA-15 silica under ultrasonic irradiation [14]. The pore diameters of the above spheres are all below 10nm. However, for many applications, such as biomacromolecule separation, drug-delivery, bio-molecular release and guest molecule encapsulation, much larger pores of materials are highly required, as well as their entirely uniform shape.

In this chapter, mesoporous silica spheres have been obtained via a two-step synthesis process by using a triblock copolymer as template in combination with a co-surfactant and co-solvent. Multi-amine-grafted mesoporous silicas SBA-15 were prepared by attaching 3-

aminopropyltriethoxysilane, *N*-2(-aminoethyl)-3-aminopropyl trimethoxysilane and (3-trimethoxysilylpropyl) diethylenetriamine via post-synthesis method. The protein adsorption properties such as equilibrium and kinetics were investigated by various models. Moreover, the release study of initial samples and modified samples also were carried out to assess application for controlled drug delivery system. These proteins were Bovine Serum Albumin (BSA), Lysozyme (LYS) and Myoglobin (MYO).

3.2. Experimental

3.2.1. Materials

The chemicals used in this chapter include most chemicals used in chapter 2. Furthermore, there were supplemental agents such as: cetyltrimethyl ammonium bromide (CTAB, Aldrich), ethanol (Junsei, absolute) and toluene (Kokusan, 97%).

3.2.2. Synthesis of spherical SBA-15

Mesoporous silica spheres were synthesized by using tetraethyl orthosilicate (TEOS) as the silica source, Pluronic P123 triblock copolymer ($PEO_{20}PPO_{70}PEO_{20}$, Aldrich) as a structure-directing agent, cetyltrimethylammonium bromide (CTAB) as the co-surfactant, and ethanol as the cosolvent. HCl was also employed to catalyze the templating process reaction. In a typical synthesis, 3 g of P123 was dissolved in 60 mL HCl (1.5 M). The desired amount of CTAB (0.6 g) and TMB were first mixed with 25 mL deionized (DI) water separately, and then the two solutions were mixed thoroughly as ethanol (100%) was added. The amount of TMB added was matched to the P123 used. The specific ratio of TMB:P123 varied depending on the pore size targeted. The resulting solution is referred to as the surfactant solution. 10 mL of TEOS was added drop by drop to the surfactant solution, and the mixture was vigorously stirred (~500 rpm) for 45 min at 35 ^{o}C. After stirring, the mixture was transferred to a heatproof

plastic bottle and stored under static condition at 75 ^{o}C and then aged at 125 ^{o}C. The white precipitate was recovered by filtration, dried at 90 ^{o}C for 24 hours, and calcined in air at from room temperature to 550 ^{o}C, with a heating rate of 1 ^{o}C/min. The temperature was held constant at 550 ^{o}C for 6 hours, the cooling rate was 5 ^{o}C/min.

3.2.3. Modification of SBA-15

The procedure to modify surface of spherical mesoporous materials SBA-15 by grafting aminopropyl groups is similar to rod-shaped SBA-15. The materials after modification are designated as S-APTES, S-AEAPS and S-TA, where APTES, AEAPS and TA are 3-aminopropyltriethoxysilane, *N*-2(-aminoethyl)-3-aminopropyltrimethoxysilane, and N^1-[3-(trimethoxysilyl)-propyl]diethylene triamine, respectively.

3.2.4. Characterization

The initial and modified spherical SBA-15 samples were characterized by XRD, nitrogen adsorption and desorption analysis, SEM, TEM and FT-IR. These characterization procedures are the same as rod-shaped SBA-15 samples.

3.2.5. Protein adsorption and release study

Protein adsorption equilibrium and release experiments were carried out similarly to the rod-shaped SBA-15 in chapter 2.

The kinetic adsorption experiments were performed in a batch at 25 ^{o}C. In each adsorption experiment, 200 mg of the different adsorbents was suspended in 50 mL of the protein solution with 2 mg/mL concentration. The suspensions were continuously shaken with a speed of 250 rpm. The concentrations of proteins at different time intervals were analyzed using UV-spectrophotometer. For all experiments concerning adsorption and kinetic, pH values

of buffer solutions were 4.8 for BSA, 7.0 for LYS and MYO.

3.3. Results and discussion

3.3.1. Characterization of spherical SBA-15

XRD patterns

The synthesized spherical SBA-15 samples S1, S2 and S3 were characterized by XRD. Fig. 3.1 shows the XRD patterns of these samples, which shows that spherical SBA-15 exhibited single diffraction peaks, characteristic of mesoporous materials with a pore structure lacking long-range order. After attaching amine functional group onto the silica surface, the XRD pattern is changed. There is no peak in the XRD pattern of S2-AEAPS and this is consistent with literatures [5,35].

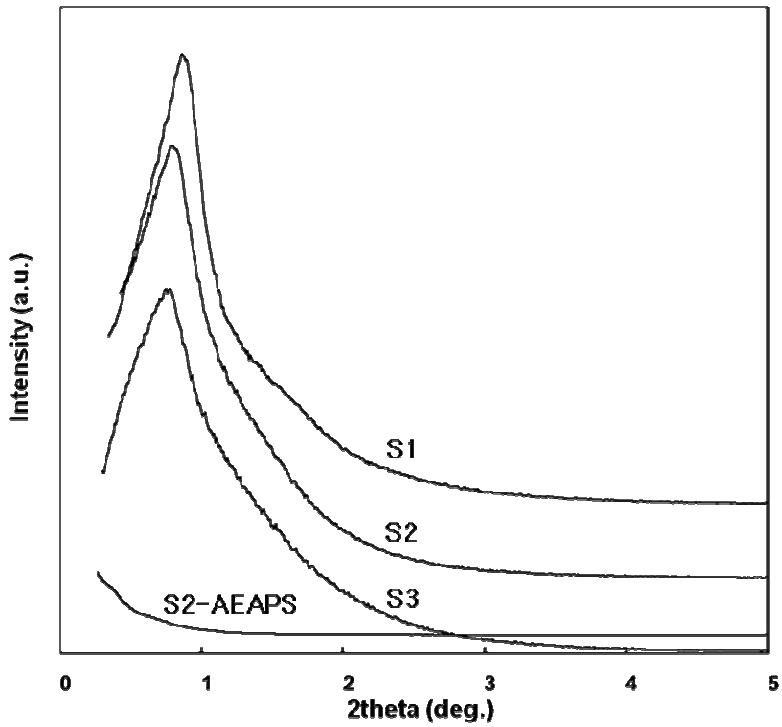

Fig. 3.1. XRD patterns of spherical SBA-15.

SEM

CTAB was used as a co-surfactant while ethanol was used as co-solvent to synthesize spherical SBA-15 particles. Zhao et al. [9] synthesized various morphological structures using difference synthesis conditions. The morphology of the SBA-15 was said to be controlled by condensation rate of silica species (pH and silica source), stirring rate, micelle shape, and inorganic species present. The morphology of these materials is highly dependent on the energy of local curvature. The attainment of a lower local energy of curvature will result in a more curved morphology. TEOS was selected as the silica source to reduce the local energy of curvature; TEOS has slower condensation rates as compared to TMOS.

A. Katiyar et al. [36] showed that the use of higher amount of co-surfactant CTAB does not have a significant effect on the morphology of the particles. Also, the particle size of the spherical SBA-15 was not significantly affected. However, the yield of spherical particles decreased as the CTAB concentration was increased. It has been proposed that in the absence of co-surfactant, the surfactant S^0 and positively charged silica I^+ interact in an acidic environment mediated by an ionic pair $S^0H^+X^-I^+$. This hydrogen bonded interaction is relatively weak and allows the preparation of porous solids with different shapes. The use of CTAB allows adjustment of the shape and size of the particles during the synthesis. In the absence of CTAB we have obtained particles with undefined shape and size.

Ethanol plays a very important role in determining the characteristics of the SBA-15 particles [28]. To examine the effect of ethanol on the morphology of the product, a synthesis was performed in the absence of ethanol with other reaction conditions kept similar to that for E1. The resulting product exhibited a mixture of lots of irregular particles and some microspheres. The addition of the cosolvent ethanol may decrease the polarity of the solvent

and thus decrease the rate of nucleation and growth of the mesostructured products because of the slower TEOS hydrolysis and mesostructure assembly, which could contribute to the formation of silica spheres with smooth surfaces. It has been reported that uniform mesoporous silica microspheres can be obtained by using alkylamine as a template and ethanol as an auxiliary solvent, and a remarkable improvement of the spherical morphology has been attributed to the presence of ethanol [29]. It is noted that mesoporous SBA-15 particles obtained by using P123 as the template and CTAB as the cosurfactant did not show a perfect spherical morphology [9], which suggested that the cosolvent ethanol played an important role in the formation of perfect spheres of mesoporous silica. However, an increased amount of ethanol destroys the spherical structure as well as the mesostructure (Fig. 3.2).

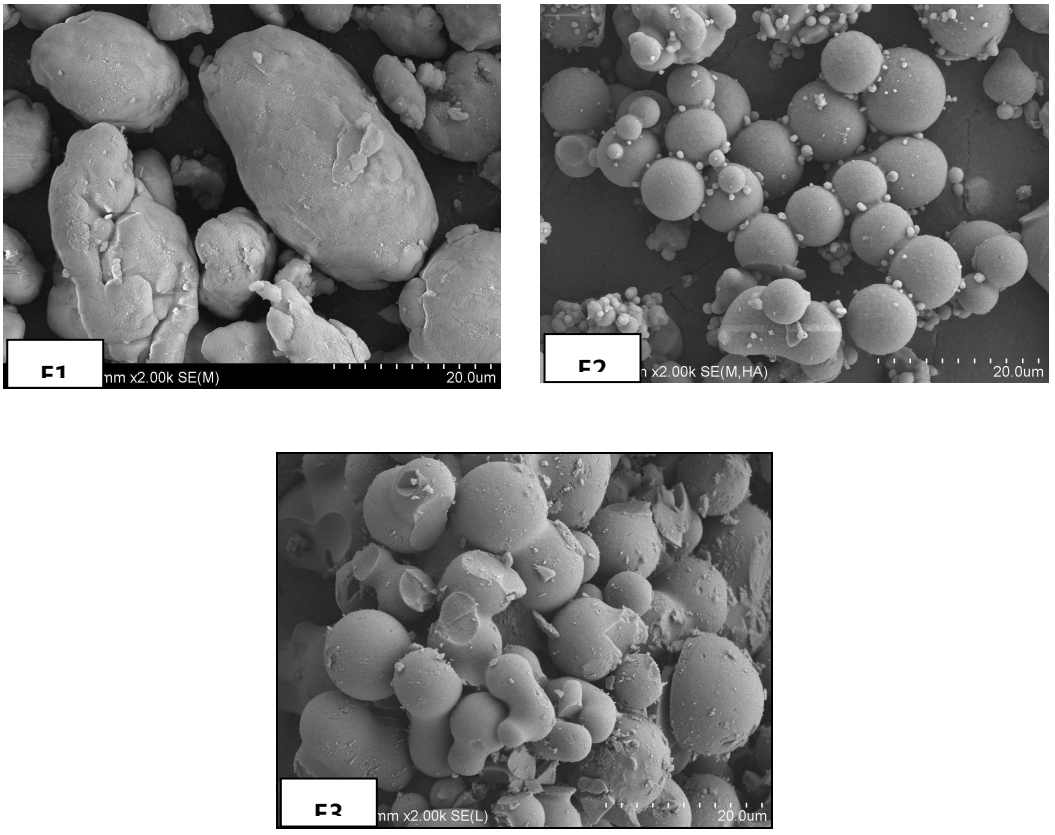

Fig. 3.2. SEM images show effect of ethanol on morphology of spherical SBA-15: (E1) absence of ethanol; (E2) ethanol 20 mL; (E3) ethanol 30 mL.

The addition of swelling agent increases the pore size. However, the particle morphology can be changed. Fig. 3.3 shows the change in particle morphology as the amount of swelling agent is increased and the ethanol amount is 20 mL.

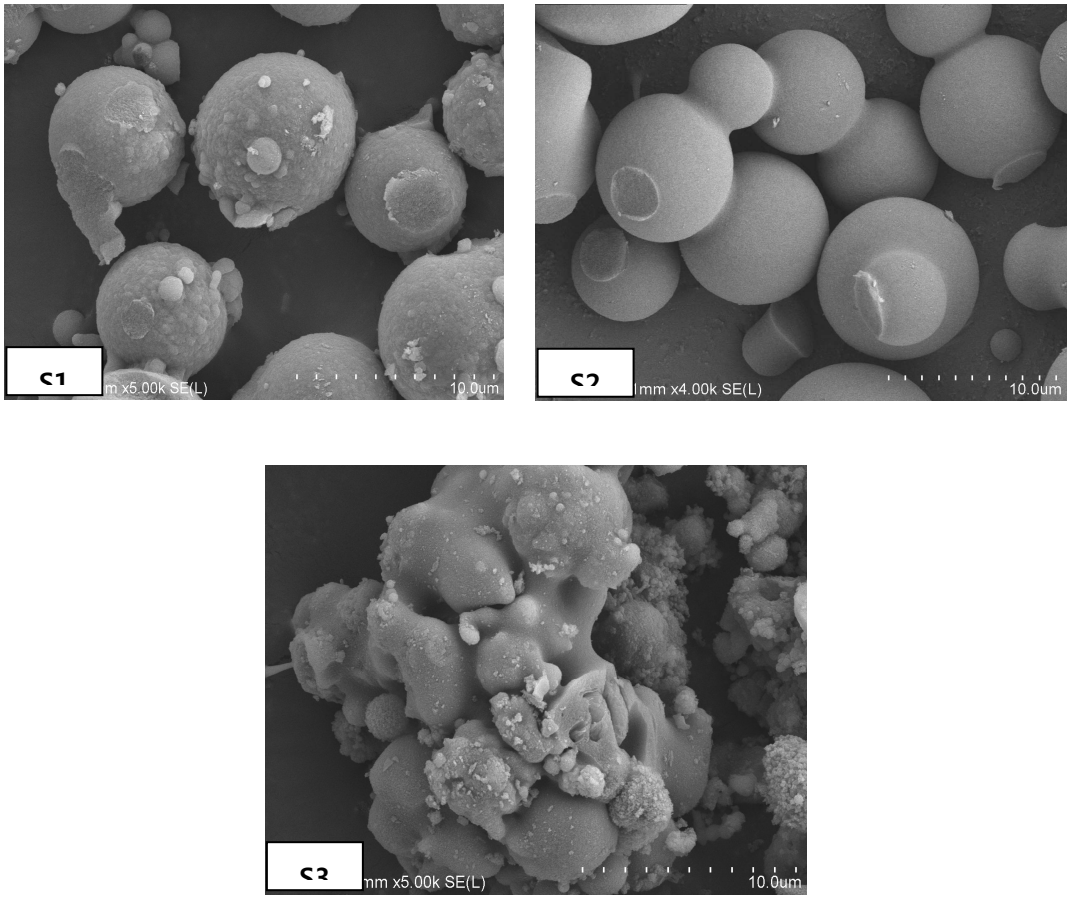

Fig. 3.3. SEM inmages showing effect of TMB on morphology of spherical SBA-15: (S1) TMB/P123 = 0.25; (S2) TMB/P123 = 0.50; (S3) TMB/P123 = 0.75.

BET

Fig. 3.4 shows the pore volume of the nitrogen physisorption isotherms of the samples S1, S2 and S3, which gives a typical irreversible type IV isotherm with a H_1 hysteresis loop as defined by IUPAC [26]. The nitrogen adsorption at low relative pressures (P/P_o<0.1) is accounted for by monolayer adsorption of nitrogen on the pore walls, and does not necessarily imply the presence of micropores. The sharp inflection in the P/P_o range from 0.6 to 0.9 of the isotherm is characteristic of capillary condensation within uniform mesopores, the position of which is clearly related to a diameter in the mesopore range. The pore size distribution of samples S1, S2 and S3 displayed in Fig. 3.5. was determined by the BJH method.

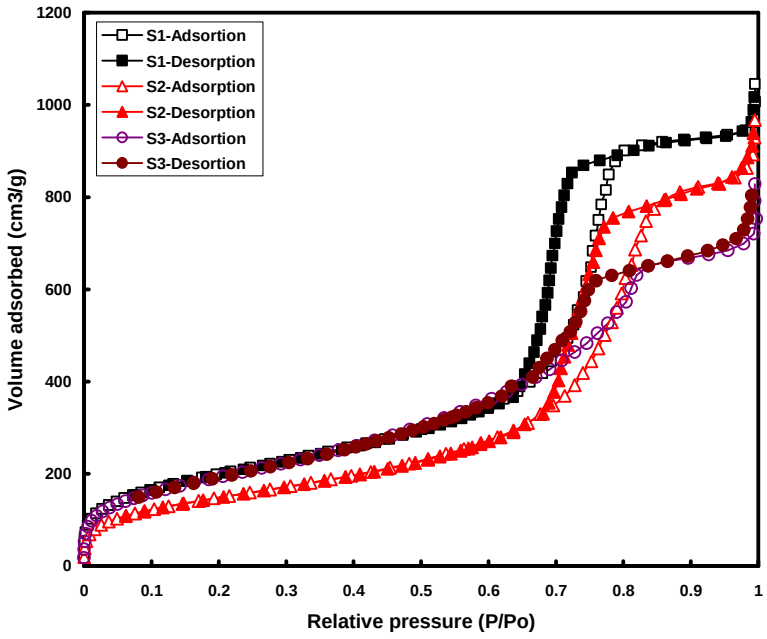

Fig. 3.4. Nitrogen adsorption and desorption isotherms of spherical SBA-15.

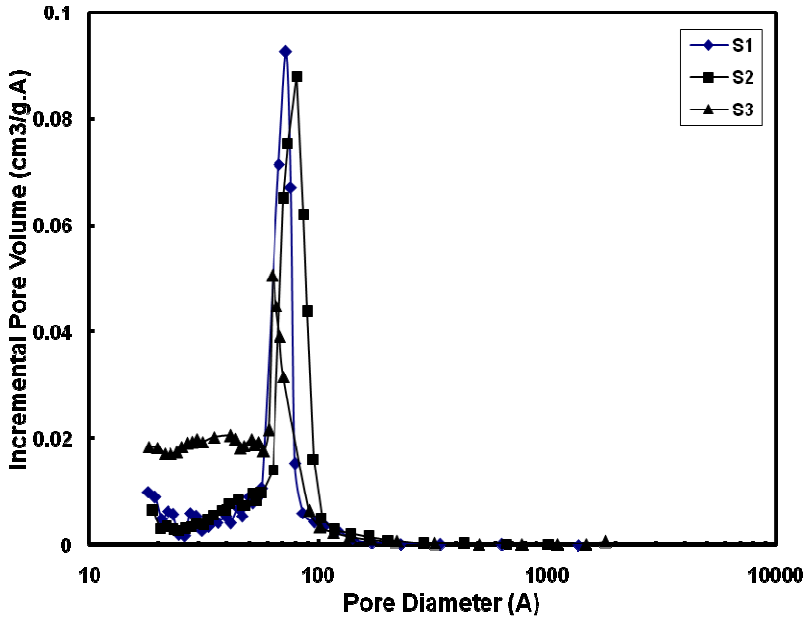

Fig. 3.5. BJH desorption pore diameter distribution patterns of synthesized SBA-15 spheres.

The effect of swelling agent (TMB) on the properties of SBA-15 is summarized in Table 3.1. In many previous studies, the addition of swelling agent increases the pore size. This is agreement for S1 and S2, the mean pore diameter increase as the TMB amount is increased. However, as the amount of swelling agent is increased in 0.75 of TMB/P123 ratio, the pore diameter is decreased and the change in particle morphology is seen at the same time.

Table 3.1. Physical properties of synthesized SBA-15 spheres.

Sample	TMB/P123	BET surface area (m^2/g)	Mesopore volume (cm^3/g)		Mean mesopore diameter (Å)	
			BJH Ads.	BJH Des.	BJH Ads.	BJH Des.
S1	0.25	737	1.57	1.62	86	72
S2	0.50	552	1.43	1.49	92	81
S3	0.75	714	1.15	1.28	58	63

Among three samples, S2 has the largest pore size and the most clear spherical morphology, thus it had been chosen for incorporating amine groups onto the surface. The nitrogen adsorption-desorption isotherms and the corresponding BJH pore size distribution curves of the original SBA-15 sphere and functionalized samples are shown in Fig. 3.6 and Fig. 3.7, respectively. The reduction of the mesopore volume after functionalization has been observed, which is attributed to the lower affinity for N_2 of the grafted surface as well as to less accessibility to the mesopores. The uniform pore size distribution was retained for aminosilane-modified SBA-15. The mean pore diameter of amine functionalized SBA-15 were lower than those of the SBA-15 support (S2), indicating that aminosilanes were anchored on pore walls of SBA-15. The mean pore diameter of APTES-, AEAPS- and TA-modified SBA-15 decreased in the following order: APTES > AEAPS > TA. This order was in accordance with the order molecular sizes of respective aminosilanes. The physical properties of original and modified samples are summarized in the Table 3. 2.

Table 3. 2. Physical properties of original and amine functionalized SBA-15 spheres.

Sample	BET surface area (m^2/g)	Mesopore volume (cm^3/g)		Mean mesopore diameter (Å)	
		BJH Ads.	BJH Des.	BJH Ads.	BJH Des.
S2	552	1.43	1.49	92	81
S2-APTES	522	1.00	1.04	53	49
S2-AEAPS	466	1.00	1.01	49	46
S2-TA	486	0.77	0.81	47	46

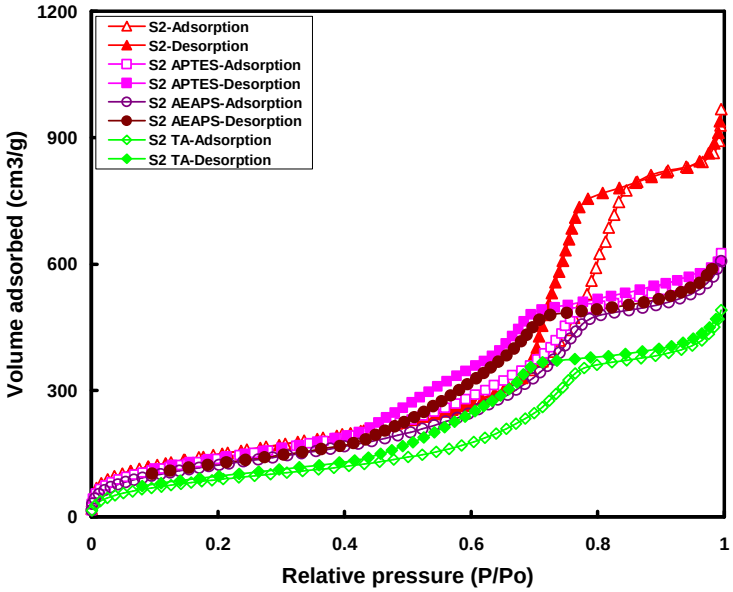

Fig. 3.6. Nitrogen adsorption and desorption isotherms of original and amino-functionalized SBA-15 spheres.

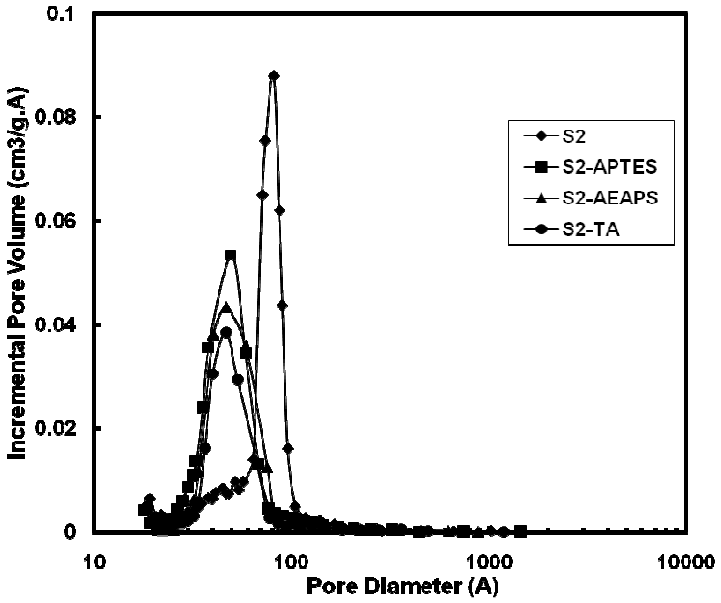

Fig. 3.7. BJH desorption pore diameter distribution patterns of original and amino-

functionalized SBA-15 spheres.

TEM

A typical high-resolution TEM image of the SBA-15 spheres is presented in Fig. 3.8 (a), which shows irregularly aligned mesopores with relatively uniform pore sizes. This result is in good agreement with the related XRD and N_2 adsorption results. It has been documented that mesoporous silica with a hexagonal structure can be prepared via the co-assembly of either CTAB or P123 with cationic silica species in acid condition [3,33]. Mesoporous silica products obtained in the presence of single CTAB or P123 under the current synthesis conditions have not exhibited the spherical morphology, suggesting that the presence of both CTAB and P123 is essential for the formation of the mesoporous silica spheres. In the present synthesis, the molar ratio between CTAB and P123 is about 3 but the weight ratio between them is actually very low (1/5). Therefore, the polymer P123 contributes largely to the final mesopores whereas the surfactant CTAB mainly plays a role of co-surfactant. The fact that the mesoporous silica obtained by using the mixed P123-CTAB templates shows a monodisperse rather than a bimodal pore size distribution indicates that the mesopores could be formed by the co-assembly of the mixed P123-CTAB micelles with cationic silica species (Fig. 3.9). Since the mixed P123-CTAB micelles are not so uniform as the single P123 or CTAB micelles, the final mesopore structure tends to lack a long-range hexagonal order.

The TEM image of modified sample shows the significant difference in the spacing between channels from the original SBA-15. It is referred to the amine group coated on the surface of original SBA-15 spheres (Fig. 3.8 (b)).

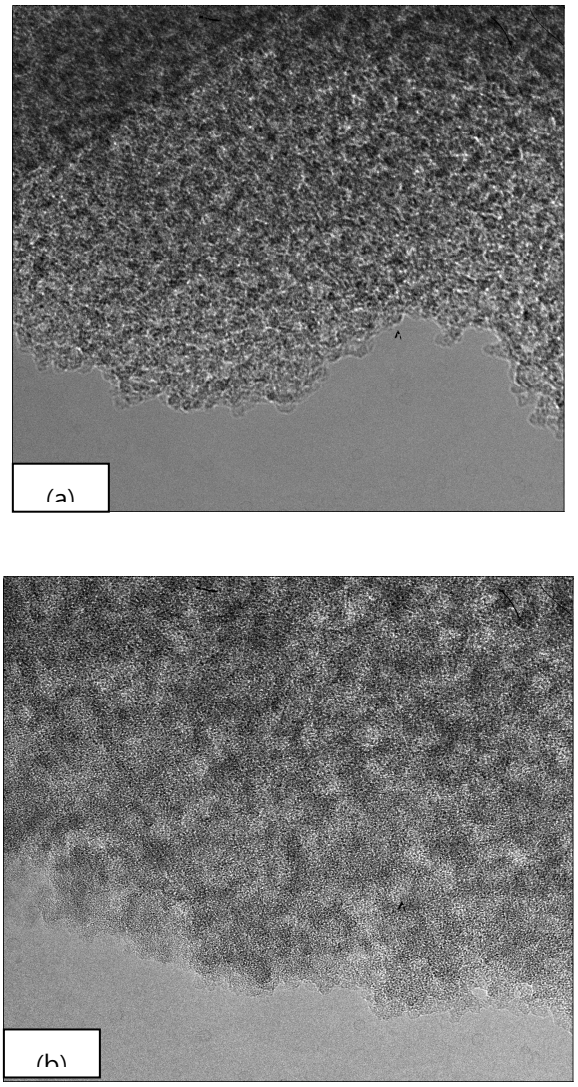

Fig. 3.8. TEM images of original (a) and amine-functionalized SBA-15 spheres (b).

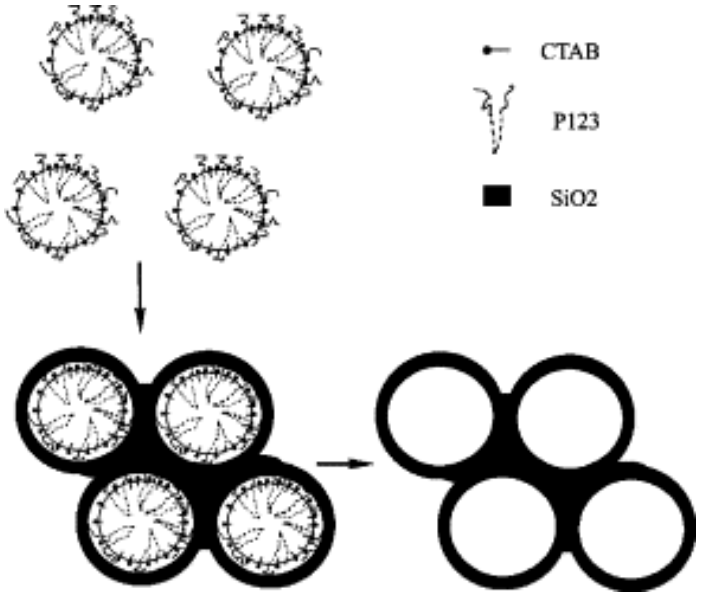

Fig. 3.9. Schematic diagram shows the assembly of the mixed P123-CTAB micelles and the formation of the final mesopore structure.

FT-IR

Fig. 3.10 shows the infrared spectra of SBA-15 spheres before (S2) and after modification (S2-APTES, S2-AEAPS and S2-TA). There are several bands appearing in the amino-functionalized SBA-15. In fact, it is difficult to determine the functional group $–NH_2$ attached on the surface mesoporous material by observing peak around 3460 cm^{-1} because the band of $–NH_2$ overlaps with that of O-H stretching vibration [5]. The appearance of peaks at 2937 and 1560 cm^{-1} corresponds to the C-H stretching and N-H (primary amine) bending vibration, respectively and this confirms the presence of $–Si(CH_2)_3NH_2$ functional groups on the wall surface.

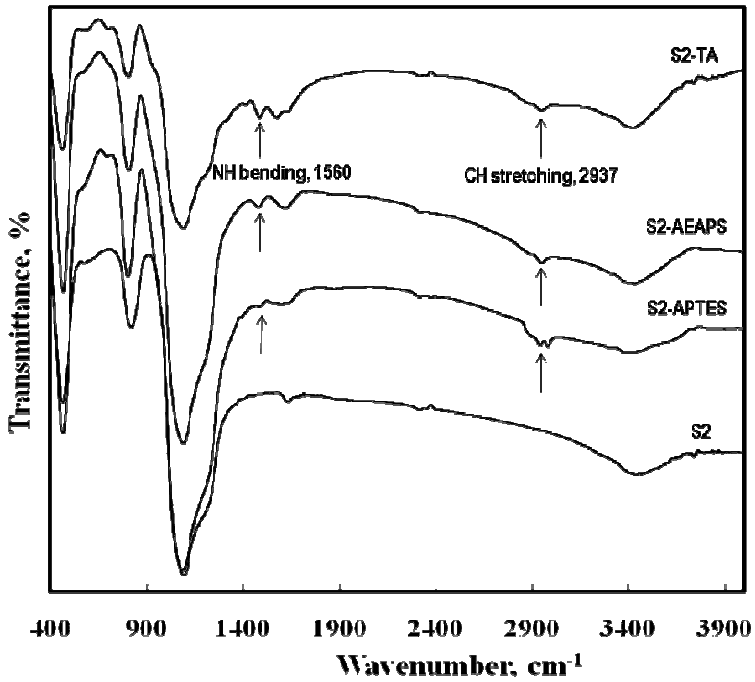

Fig. 3.10. Infrared spectra of SBA-15 spheres before (S2) and after modification (S2-APTES, S2-AEAPS and S2-TA).

3.3.2. *Protein adsorption and release study*

The isoelectric point is the pH value in solution at which the sum of charges on the protein is zero. The protein molecular is positively charged at a pH below the pI, on the contrary it is negatively charged at a pH above the pI. Because the pI values of BSA and MYO are 4.8 and 7.0, respectively, the protein adsorption experiments were carried out at 25 ^{o}C and pH values of 4.8 and 7.0. However, there is an exception for LYS concerning breakableness of SBA-15 in alkali solution. Although the pI of LYS is 11, the pH value of buffer solution used for LYS adsorption experiment is 7. This was also carried out in previous study [36].

We have also used equations (1), (2), and (3) presented in chapter 2 to calculate isotherm data. The determined isotherm parameters of proteins on SBA-15 are listed in Table 3.3.

Table 3.3. Langmuir isotherm parameters of proteins (for spherical SBA-15).

Protein	SBA-15 samples	q_m	b	*E(%)*
BSA	S2	48.62	0.66	4.08
LYS	S2	110.49	149.9	3.13
	S2-APTES	11.58	5.01	7.47
	S2-AEAPS	2.25	20.01	2.59
MYO	S2	215.4	71.08	10.05
	S2-APTES	39.50	0.41	1.52
	S2-AEAPS	79.15	0.76	4.69
	S2-TA	48.89	1.07	4.33

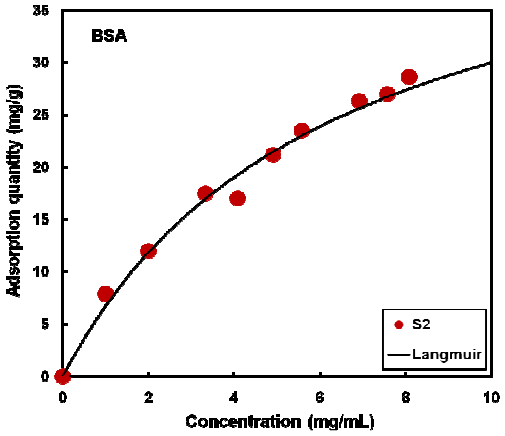

Fig. 3.11. Adsorption isotherm of BSA on original SBA-15 sphere.

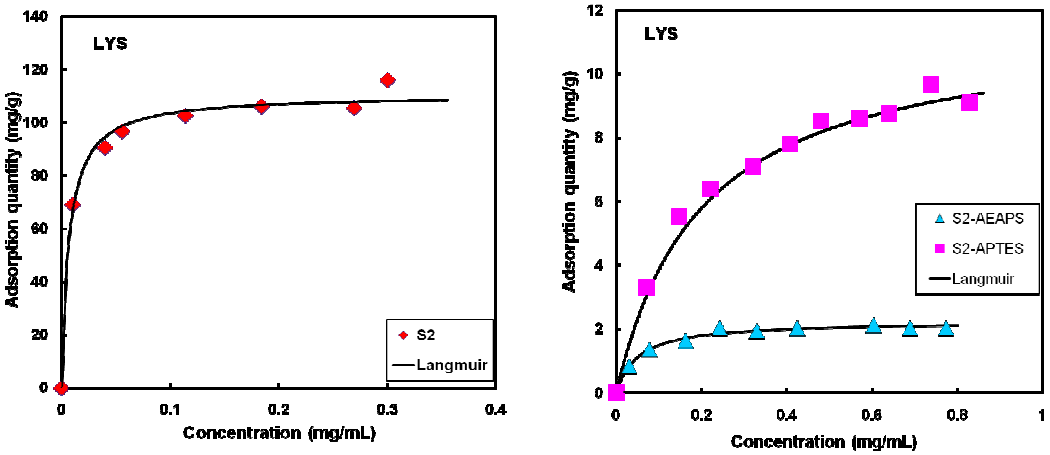

Fig. 3.12. Adsorption isotherms of LYS on amino-functionalized SBA-15 spheres.

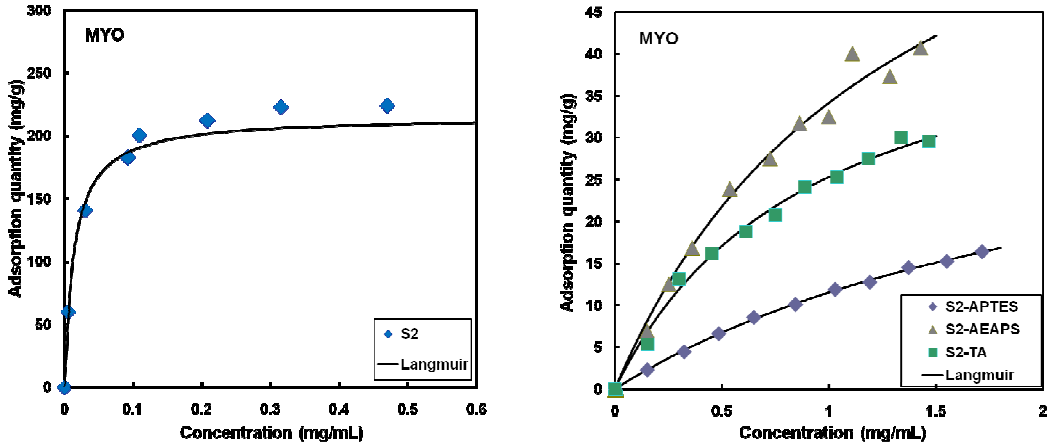

Fig. 3.13. Adsorption isotherms of MYO on amino-functionalized SBA-15 spheres.

There are some differences in adsorption capacity of SBA-15 samples between proteins (Fig. 3.11, 3.12, 3.13). The sample which has the highest adsorption capacity for all proteins is the original sample S2 due to its largest pore size and internal surface area. After attaching functional groups onto the surface, the adsorption amounts of S2-APTES, S2-AEAPS and S2-TA were decreased due to a significant decrease in pore size and surface area. Besides, all modified samples do not have adsorption capacity for BSA and S2-TA also does not have adsorption capacity for LYS. Only original SBA-15 sample (S2) has adsorption capacity for BSA, but the amount of adsorption is not as high as for LYS and MYO. Moreover, the *b* parameter expresses the weak affinity of S2 for BSA, but very high affinity for LYS and MYO. The affinity of modified samples is lower than that of original sample for LYS and MYO, too. The interactions between proteins and original SBA-15 sample S2 are both of chemical bond (covalent and electrostatic bonds) and physical bond (hydrophilic interaction), due to the presence of hydroxyl groups on the surface of SBA-15 and the functional groups of proteins. After modification via post synthesis, the hydroxyl groups on the surface of silica are partially lost because of high temperature hydrothermal treatment. Moreover, the attachment of

nonpolar and hydrophobic methyl groups in grafted chains (Si-CH_2-CH_2-CH_2-NH_2) made the surface of SBA-15 more hydrophobic and a decrease in pore size. Hence, the amount of proteins adsorbed on the amine-functionalized sample is reduced in comparison with that before modification.

The ability to control protein uptake based on size, i.e., size-selective separation, is also demonstrated in Fig. 3.14. The results of adsorption kinetics show that original S2 sample has the most rapid uptake for all proteins and can reach saturation level for 10 hours. On spherical S2 with pore size of 92 Å, the amounts of BSA, LYS and MYO adsorbed at equilibrium are around 50, 120 and 220 mg/g, respectively. The dimensions of BSA molecule is reported to be 40 Å x 40 Å x 140 Å, while the dimensions of LYS and MYO are 30 Å x 30 Å x 45 Å and 25 Å x 35 Å x 45 Å, respectively. Since the largest dimensions of BSA are larger than the pore size, this molecule can be expected to be excluded from the pores; the small amount adsorbed is expected to be located on the external surface of the particles or at the pore mouths. In contrast, since the largest dimension of LYS and MYO is approximately a half of the pore diameter of S2, these molecules were adsorbed with high capacity. For all modified SBA-15 samples, the uptake rate for LYS is faster than that for MYO. The saturation amounts are different for each modified sample because of difference in pore size and affinity as expressed above.

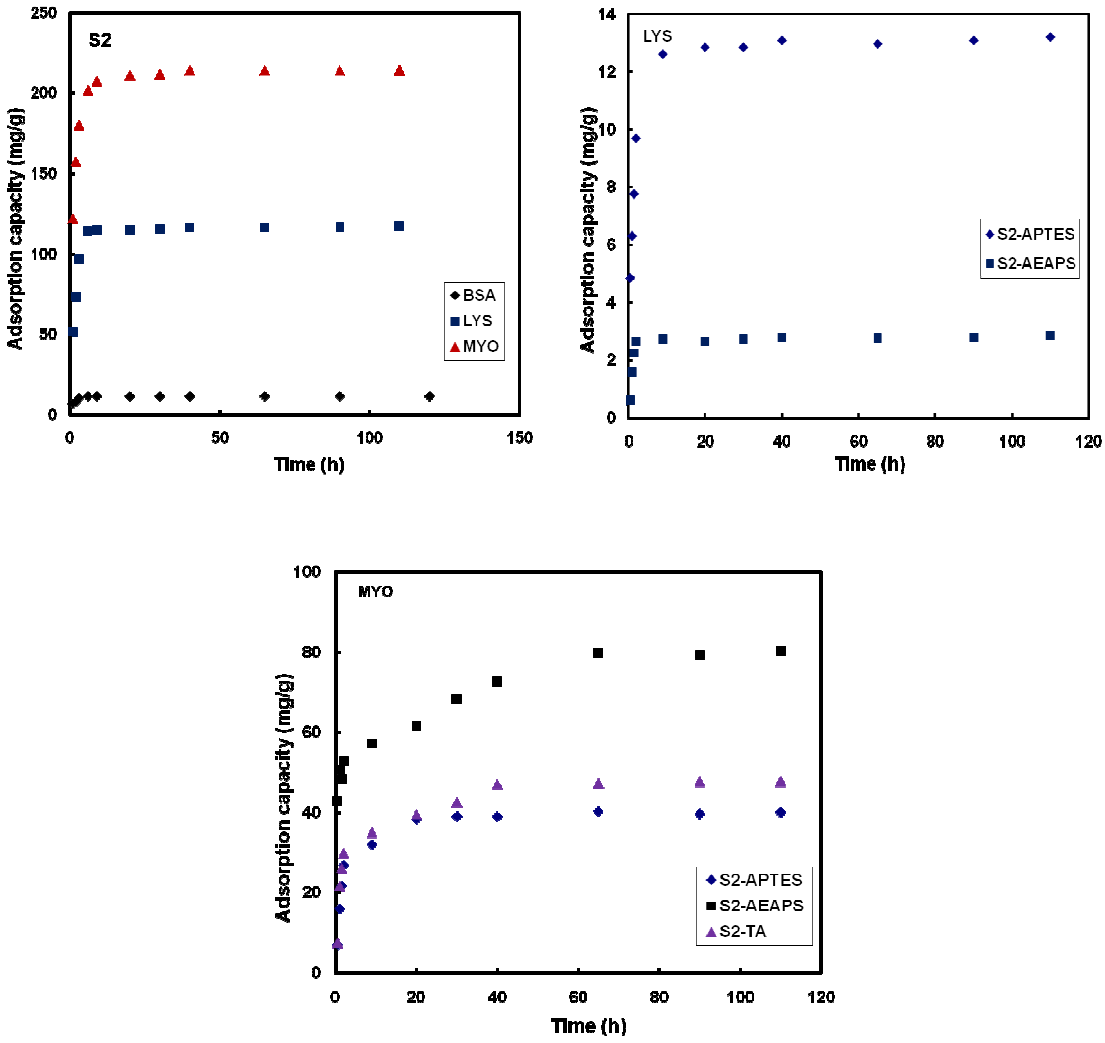

Fig. 3.14. Protein adsorption kinetics of spherical SBA-15 samples.

The release study was performed for LYS and MYO. Although the adsorption capacity of S2 was highest among all samples, the amount released by functionalized samples was higher than that of S2 for LYS and TA (Fig. 3.15). Especially, S2-AEAPS has highest release amount. As it has been stated, the interaction between the adsorbed molecules and the functionalized SBA-15 surface is governed by both hydrophobic and electrostatic interaction. In addition, there are some differences in nature of these interactions among SBA-15 samples. Hence, the release amounts are different from each sample. Generally, S2-AEAPS is a very good candidate to apply in controlled drug delivery system.

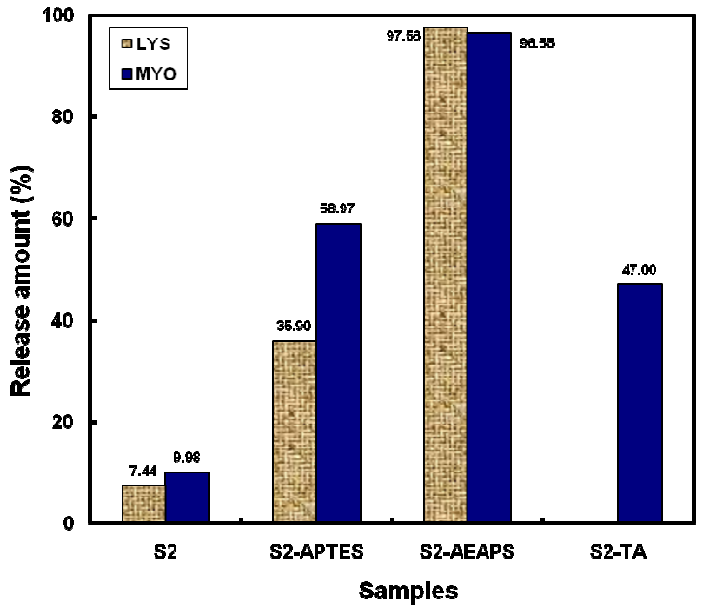

Fig. 3.15. Release experiment for original and modified SBA-15 spheres.

The protein release profiles from mesoporous material SBA-15 as a function of time are shown in Fig. 3.16. Generally, the release curves can be separated into two parts: an initial fast release followed by a slow release pattern. The fast release is mainly caused by the dissolution of the proteins which is physically adsorbed in SBA-15, and the slow release may be attributed to the chemically adsorbed proteins.

The S2-AEAPS exhibited 62 wt% of LYS pronouncing the initial burst release within 5.5 h, 95 wt% has been released within 30 h, and 98 wt% has been released within 90 h. Although the release amounts of LYS from S2 and S2-APTES are lower than that from S2-AEAPS, the cumulative release rates of LYS from S2 and S2-APTES are faster than that from S2-AEAPS. Namely, the fast initial burst release of LYS from S2 and S2-APTES are 30 wt% and 5.5 wt%, respectively, within 3 h.

For MYO, the cumulative release rates from S2 and S2-APTES are faster than that from S2-AEAPS and S2-TA. The fast initial burst release of MYO from S2 and S2-APTES is within 5 h, whereas this is within 35 h for S2-AEAPS and S2-TA.

Different release mechanisms, either surface or time dependent, were also observed as a consequence of the diverse drug-matrix governing interaction. Thus, a range of different adsorption and release kinetics are here presented, which is of importance to achieve the desired dosage of a specific protein. These results are of great interest for designing silica-based materials for the adsorption and controlled release of proteins.

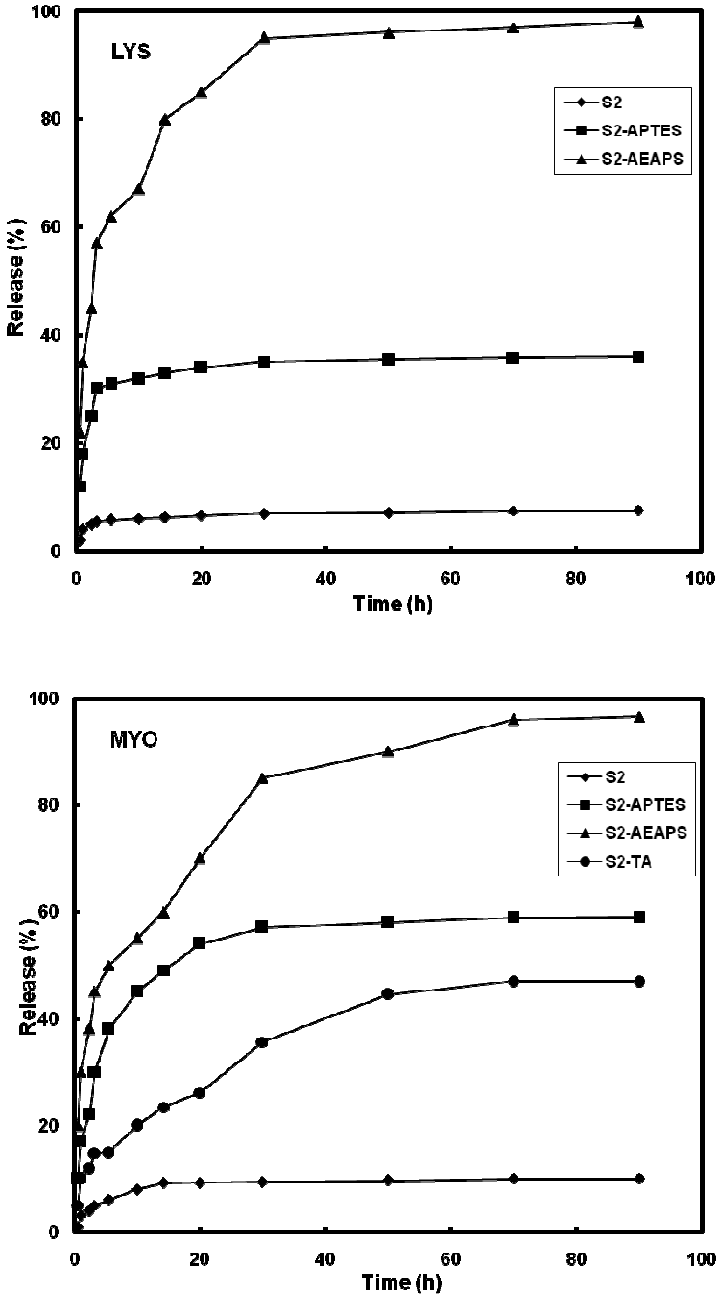

Fig. 3.16. Release profiles of LYS and MYO from spherical SBA-15 samples.

3.4. Conclusion

In this chapter, we have made the SBA-15 samples with spherical morphology. Ethanol plays a very important role in determining the characteristics of the SBA-15 particles. The amount of swelling agent was investigated in order to find the best condition ensuring that the SBA-15 sample has the largest pore size as well as the best complete spherical morphology (S2). In addition, the surface characteristics of S2 can be modified by incorporating amine functional groups via post synthesis method. The adsorption equilibrium and kinetics of BSA, LYS and MYO on conventional and amine-modified SBA-15 samples were performed. The original SBA-15 has the highest adsorption capacity for all proteins due to its largest pore size and internal surface area. Langmuir equation was applied for fitting the isotherm data. It was found that the adsorbed proteins can be readily desorbed in the neutral solution on amine-modified samples, too. Among amino-functionalized samples, S2-AEAPS has the highest release amount (97.56% for LYS and 96.55% for MYO). The release kinetics experiments were also carried out. These results are of great interest for designing silica-based materials for the controlled drug delivery system.

CHAPTER 4. OVERALL CONCLUSIONS

Based on morphology of SBA-15 particles, each has its own synthesis procedure and characteristics, resulting in different adsorption capacity as well as application in drug delivery system. This study focused on synthesis mesoporous material SBA-15 with both rod-shaped and spherical morphology.

The rod-shaped SBA-15 sample with the large pore size has been synthesized by using swelling agent under certain conditions, i.e. at high aging temperature and prolonged aging time. In addition, the surface characteristics of SBA-15 can be modified by incorporating amine functional groups via post synthesis method. The adsorption equilibrium of BSA, LYS and MYO on conventional and amine-modified SBA-15 reaches the maximum value at the pI of proteins because the lateral repulsion between adsorbed proteins is minimal. The original rod-shaped SBA-15 has the highest adsorption capacity for all proteins due to its largest pore size and internal surface area. The isotherm data fitted very well with Langmuir equation.

The SBA-15 samples with spherical morphology had synthesized, too. Ethanol plays a very important role in determining the characteristics of the SBA-15 particles. The amount of swelling agent was investigated in order to find the best condition ensuring that the SBA-15 sample has the largest pore size as well as the best complete spherical morphology (S2). In addition, the surface characteristics of S2 can be modified by incorporating amine functional groups via post synthesis method. The adsorption equilibrium and kinetics of BSA, LYS and MYO on conventional and amine-modified SBA-15 samples were performed. The original SBA-15 has the highest adsorption capacity for all proteins due to its largest pore size and internal surface area. Among amino-functionalized samples, S2-AEAPS has the highest release amount (97.56% for LYS and 96.55% for MYO).

The release kinetics experiments were also carried out for amino-functionalized SBA-15 samples with both rod-shaped and spherical morphology. It was also found that the adsorbed proteins can be readily desorbed in the neutral solution on amine-modified samples. Thus, the modified samples can be applied for controlled drug delivery system.

REFERENCES

1. J.S. Beck, J.C. Vartuli, W.J. Roth, M.E. Leonowicz, C.T. Kresge, K.D. Schmitt, C.T.W. Chu, D.H. Olson, E.W. Sheppard, S.B. McCullen, J.B. Huggins, J.L. Schelenker (1992) A new family of mesoporous molecular sieves prepared with liquid crystal templates. *J. Am. Chem. Soc*. 114, 10834-10843.

2. C.T. Kresge, M.E. Leonowicz, W.J. Roth, J.C. Vartuli, J.S. Beck (1992) Ordered mesoporous molecular sieves synthesized by a liquid-crystal template mechanism. *Nature* 359, 710-712.

3. D. Zhao, Q. Huo, J. Feng, B.F. Chmelka, G.D. Stucky (1998) Nonionic Triblock and Star Diblock Copolymer and Oligomeric Surfactant Syntheses of Highly Ordered, Hydrothermally Stable, Mesoporous Silica Structures. *J. Am. Chem. Soc*. 120, 6024-6036.

4. L. Ji, A. Katiyar, N. Pinto, P. Smirniotis (2005) Al-MCM-41 sorbents for bovine serum albumin: relation between Al content and performance. *Microporous and Mesoporous Materials* 75, 221-229.

5. T.P.B. Nguyen, J.W. Lee, H. Moon (2008) Synthesis of functionalized SBA-15 with ordered large pore size and its adsorption properties of BSA. *Microporous and Mesoporous Materials* 110, 560-569.

6. K. Kosuge, T. Sato, N. Kikukawa, M. Takemori (2004) Morphological Control of Rod- and Fiberlike SBA-15 Type Mesoporous Silica Using Water-Soluble Sodium Silicate *Chem. Mater*. 16, 899-905.

7. A. Sayari, B.H. Han, Y. Yang (2004) Simple Synthesis Route to Monodispersed SBA-15 Silica Rods. *J. Am. Chem. Soc*. 126, 14348-14349.

8. C. Yu, J. Fan, B. Tian, D. Zhao, G.D. Stucky (2002) High-Yield Synthesis of Periodic Mesoporous Silica Rods and Their Replication to Mesoporous Carbon Rods. *Adv. Mater*. 14, 1742-1745.

9. D. Zhao, J. Sun, Q. Li, G.D. Stucky (2000) Morphological Control of Highly Ordered Mesoporous Silica SBA-15. *Chem. Mater.* 12, 275-279.

10. Z. Ko´nya, J. Zhu, A. Szegedi, I. Kiricsi, P. Alivisatos, G.A. Somorjai (2003) Synthesis and characterization of hyperbranched mesoporous silica SBA-15. *Chem. Commun.* 314-315.

11. J. Zhao, F. Gao, Y. Fu, W. Jin, P. Yang, D. Zhao (2002) Biomolecule separation using large pore mesoporous SBA-15 as a substrate in high performance liquid chromatography. *Chem. Commun*. 752-753.

12. K.W. Gallis, J.T. Araujo, K.J. Duff, J.G. Moore, C.C. Landry (1999) The Use of Mesoporous Silica in Liquid Chromatography. *Adv. Mater*. 11, 1452-1455.

13. C. Boissière, M. Kümmel, M. Persin, A. Larbot, E. Prouzet (2001) Spherical MSU-1 Mesoporous Silica Particles Tuned for HPLC. *Adv. Funct. Mater*. 11, 129-135.

14. S.K. Lee, J. Lee, J. Joo, T. Hyeon, H.-I. Lee, C.-H. Lee, W. Choi (2003) Rapid Sonochemical Synthesis of Spherical-shaped Mesoporous SBA-15 silica and Ti-incorporated SBA-15 silica Materials. *J. Ind. Eng. Chem*. 9, 83-88.

15. K. Albert, E. Bayer (1991) Characterization of bonded phases by solid-state NMR spectroscopy. *J. Chromatography* 544, 345-370.

16. K. Albert, R. Brindle, J. Schmid, B. Buszewski, E. Bayer (1994) CP/MAS NMR Investigations of Silica Gel Surfaces Modified With Aminopropylsilane. *Chromatographia* 38, 283-230.

17. G.S. Caravajal, D.E.Leyden, G.R. Quinting, G.E. Maciel (1988) Structural characterization of (3-aminopropyl)triethoxysilane-modified silicas by silicon-29 and carbon-13 nuclear magnetic resonance. *Anal. Chem*. 60, 1776-1786.

18. J.J. Yang, I.M. El-Nahhal, I.S. Chuang, G.E. Maciel (1997) Synthesis and solid-state NMR structural characterization of polysiloxane-immobilized amine ligands and their metal complexes. *J. Non-Cryst. Solids* 209, 19-39.

19. C.A. Fyfe, G.C. Gobbi, G.J. Kennedy (1985) Quantitatively reliable silicon-29 magic-angle spinning nuclear magnetic resonance spectra of surfaces and surface-immobilized species at high field using a conventional high-resolution spectrometer . *J. Phys. Chem*. 89, 277-281.

20. K.C. Vrancken, P. Vander Voort, K. Possemiers, E.F. Vansant (1995) Surface and Structural Properties of Silica Gel in the Modification with γ-Aminopropyltriethoxysilane. *J. Colloid Interface Sci*. 174, 86-91.

21. L. Zhang, C. Yu, W. Zhao, Z. Hua, H. Chen, L. Li, J. Shi (2007) Preparation of multi-amine-grafted mesoporous silicas and their application to heavy metal ions adsorption. *J. Non-Crys. Solids* 353, 4055-4061.

22. N. Hiyoshi, K. Yogo, T. Yashima (2005) Adsorption characteristics of carbon dioxide on organically functionalized SBA-15. *Microporous and Mesoporous Materials* 84, 357-365.

23. H.H.P. Yiu, P.A. Wright, N.P. Botting (2001) Enzyme immobilisation using SBA-15 mesoporous molecular sieves with functionalised surfaces. *J. Mol. Catal*. 15, 81-92.

24. S. W. Song, K. Hidajat, S. Kawi (2005) Functionalized SBA-15 Materials as Carriers for Controlled Drug Delivery: Influence of Surface Properties on Matrix-Drug Interactions. *Langmuir* 21, 9568-9575.

25. Y. Wang, M. Noguchi, Y. Takahashi, Y. Ohsuka (2001) Synthesis of SBA-15 with different pore sizes and the utilization as supports of high loading of cobalt catalysts. *Catal. Today* 68, 3-9.

26. K.S.W. Sing, D.H. Everett, R.A.W. Haul, L. Moscow, R.A. Pierotti, J. Rouquerol and T. Siemieniewska (1985) Reporting Physisorption data for Gas/Solid systems with Special Reference to the Determination of Surface Area and Porosity. *Pure & Appl. Chem*. 57, 603-619.

27. A. Katiyar, L. Ji, P. Smirniotis, N.G. Pinto (2005) Protein adsorption on the mesoporous molecular sieve silicate SBA-15: effects of pH and pore size. *J. Chromatogr.* A 1069, 119-126.

28. Y. Ma, L. Qi, J. Ma, Y. Wu, O. Liu, H. Cheng (2003) Large-pore mesoporous silica spheres: synthesis and application in HPLC. *Colloids Surf. A: Physicochem. Eng. Aspects* 229, 1-8.

29. K. Kosuge, P.S. Singh (2001) Rapid Synthesis of Al-Containing Mesoporous Silica Hard Spheres of 30-50 μm Diameter. *Chem. Mater*. 13, 2476-2482.

30. J.L. Blin, C. Otjacques, G. Herrier and S. Bao-Lian (2000) Pore Size Engineering of Mesoporous Silicas Using Decane as Expander *Langmuir* 16, 4229-4236.

31. M. Kruk, M. Jaroniec, A. Sayari (2000) New insights into pore-size expansion of mesoporous silicates using long-chain amines. *Microporous and Mesoporous Materials* 35, 545-553.

32. T. Kimura, Y. Sugahara and K.J. Kuroda (1998) Synthesis of mesoporous aluminophosphates using surfactants with long alkyl chain lengths and triisopropylbenzene as a solubilizing agent. *Chem. Commun.* 55, 559-560.

33. J.Y. Ying, C.P. Mehnert, M.S. Wong (1999) Synthesis and Applications of

Supramolecular-Templated Mesoporous Materials. *Angew. Chem. Int. Ed.* 38, 56-77.

34. M. Vallet-Regi, F. Balas, M, Colilla, M. Manzano (2007) Bone-regenerative bioceramic implants with drug and protein controlled delivery capability. *Prog. Solid State Chem.* xx, 1-29 (article in press).

35. X. Wang, J.C.C. Chan, Y.H. Tseng, S. Cheng (2006) Synthesis, characterization and catalytic activity of ordered SBA-15 materials containing high loading of diamine functional groups. *Microporous and Mesoporous Materials* 95, 57-65.

36. A. Katiyar, S. Yadav, P.G. Smirniotis, N.G. Pinto (2006) Synthesis of ordered large pore SBA-15 spherical particles for adsorption of biomolecules. *J. Chromatogr. A* 1122, 13-20.

37. B. Muñoz, A. Rámila, J. Pérez-Pariente, I. Díaz, and M. Vallet-Regí (2003) MCM-41 Organic Modification as Drug Delivery Rate Regulator. *Chem. Mater.* 15, 500-503.

38. I.I. Slowing, J.L. Vivero-Escoto, C.W. Wu, V.S.Y. Lin (2008) Mesoporous silica nanoparticles as controlled release drug delivery and gene transfection carriers. *Advanced Drug Delivery Reviews* 60, 1278-1288.

39. N. Li, X. Li, W. Wang, W. Geng, S. Qiu (2006) Blue-shifting photoluminescence of Tris (8-hydroxyquinoline) aluminium encapsulated in the channel of functionalized mesoporous silica SBA-15. *Mater. Chem. Phys.* 100, 128-131.

ACKNOWLEDGEMENT

I would like to express the deep gratitude to Prof. Sun-Il Kim, my major advisor, for always believing in, guiding and supporting me throughout my Master's program.

I wish to thank to Prof. Jae-Wook Lee very much for his whole-hearted advising and guiding for me to complete my research.

I also would like to thank to Dr. Sung-Hee Roh so much for her sentiments and help in my life and study since I have come to Korea.

Thanks sincerely all members in Chemical Process Laboratory II and Department of Chemical Engineering in Chosun University for their kind help and sharing, especially Mr. Kyung-Jun Hwang. They have always made me happy and jolly.

Thanks my lovely family, my colleagues in Vietnam and all Korean and Vietnamese friends for their love and encouragement!

Gwangju, December 5, 2008.

Pham Thi Tra

저작물 이용 허락서					
학 과	Chemical Engineering	학 번	20077710	과 정	Master
성 명	한글: 팜티트라		영문 : Pham Thi Tra		
주 소	Department of Chemical Engineering, Chosun University				
연락처	E-MAIL : htra26112002@gmail.com				
논문제목	한글 : Aminosilanes를 함침한 기능성 SBA-15 나노 입자의 단백질의 흡착 및 탈착 특성 영어 : Adsorption and Release Properties of Proteins on SBA-15 Nanoparticles Functionalized with Aminosilanes				

본인이 저작한 위의 저작물에 대하여 다음과 같은 조건아래 -조선대학교가 저작물을 이용할 수 있도록 허락하고 동의합니다.

- 다 음 -

1. 저작물의 DB구축 및 인터넷을 포함한 정보통신망에의 공개를 위한 저작물의 복제, 기억장치에의 저장, 전송 등을 허락함

2. 위의 목적을 위하여 필요한 범위 내에서의 편집·형식상의 변경을 허락함. 다만, 저작물의 내용변경은 금지함.

3. 배포·전송된 저작물의 영리적 목적을 위한 복제, 저장, 전송 등은 금지함.

4. 저작물에 대한 이용기간은 5년으로 하고, 기간종료 3개월 이내에 별도의 의사표시가 없을 경우에는 저작물의 이용기간을 계속 연장함.

5. 해당 저작물의 저작권을 타인에게 양도하거나 또는 출판을 허락을 하였을 경우에는 1개월 이내에 대학에 이를 통보함.

6. 조선대학교는 저작물의 이용허락 이후 해당 저작물로 인하여 발생하는 타인에 의한 권리 침해에 대하여 일체의 법적 책임을 지지 않음

7. 소속대학의 협정기관에 저작물의 제공 및 인터넷 등 정보통신망을 이용한 저작물의 전송·출력을 허락함.

동의여부 : 동의(o) 반대( )

2009년 2월 일

저작자: Pham Thi Tra (인)

조선대학교 총장 귀하